Theriogenology 208 (2023) 28–42

Contents lists available at ScienceDirect

Theriogenology

journal homepage: www.theriojournal.com

Ovine fertility by artificial insemination in the breeding season could be affected by intraseasonal variations in ram sperm proteomic profile

Marta Neila-Montero [a, b, 1], Mercedes Alvarez [a, b, 1], Marta F. Riesco [a, c, *], Rafael Montes-Garrido [a, b], Cristina Palacin-Martinez [a, b], Antonio Silva-Rodríguez [d], Francisco E. Martín-Cano [e], Fernando J. Peña [e], Paulino de Paz [a, c], Luis Anel [a, b], Luis Anel-Lopez [a, f]

[a] Itra-ULE, INDEGSAL, University of León, León, Spain
[b] Animal Reproduction and Obstetrics, Department of Veterinary Medicine, Surgery and Anatomy, University of León, León, Spain
[c] Cellular Biology, Department of Molecular Biology, University of León, León, Spain
[d] Facility of Innovation and Analysis in Animal Source Foodstuffs, University of Extremadura, Cáceres, Spain
[e] Laboratory of Equine Reproduction and Equine Spermatology, Veterinary Teaching Hospital, University of Extremadura, Cáceres, Spain
[f] Anatomy, Department of Veterinary Medicine, Surgery and Anatomy, University of León, León, Spain

ARTICLE INFO

Article history:
Received 16 February 2023
Received in revised form
24 April 2023
Accepted 30 May 2023
Available online 1 June 2023

Keywords:
Cervical insemination
Cooled semen
Proteomic analysis
Seasonality
Sheep
Sperm proteome

ABSTRACT

It is important to note that seasonality could affect ram reproductive parameters, and therefore, fertility results after artificial insemination. In this work, 1) we assessed fertility rates after cervical artificial insemination of 11,805 ewes at the beginning (June 21st to July 20th) and at the end (November 20th to December 21st) of the reproductive season in the Assaf breed for the last four years, and 2) we aimed to identify male factors influencing the different reproductive success obtained depending on the time at the mating season in which ovine artificial insemination was performed. For this purpose, we evaluated certain ram reproductive and ultrasonographical parameters as well as we performed a multiparametric and proteomic sperm analysis of 6–19 rams at two very distant points in the mating season (July as Early Breeding Season –EBS– and November as Late Breeding Season –LBS–). Rutinary assessments carried out in the ovine reproduction centers (testicular volume, libido, sperm production and mass motility) showed non-significant differences ($P \geq 0.05$) between both studied times, as well as the ram ultrasonographic evaluation (Resistive and Pulsatility Index as Doppler parameters; and pixels mean gray level, and hypoechoic areas percentage and density as echotexture parameters). However, at level of sperm functionality, although sperm quality appeared non-significantly lower ($P \geq 0.05$) in the EBS, we identified a significantly different ($P < 0.05$) sperm proteomic profile between the seasonality points. The following proteins were identified with the lowest abundance in the EBS with a fold change > 4, a P = 2.40e-07, and a q = 2.23e-06: Fibrous Sheath-Interacting Protein 2, Disintegrin and Metalloproteinase Domain-Containing Protein 20-like, Phosphoinositide-Specific Phospholipase C, Tektin 5, Armadillo Repeat-Containing Protein 12 Isoform X3, Solute Carrier Family 9B1, Radial Spoke Head Protein 3 Homolog, Pro-Interleukin-16, NADH Dehydrogenase [Ubiquinone] 1 Alpha Subcomplex Subunit 8, Testis, Prostate and Placenta-Expressed Protein, and Acyl Carrier Protein Mitochondrial. In conclusion, while our basic analyses on male and sperm quality showed similar results between the beginning and the end of the breeding season, on a proteomic level we detected a lower expression of sperm proteins linked to the energy metabolism, sperm-oocyte interactions, and flagellum structure in the EBS. Probably, this different protein expression could be related to the lower fertility rate of Assaf ewes after cervical artificial insemination at this time. More importantly, sperm proteins can be used as highly effective molecular markers in predicting sperm fertilization ability related to intraseasonal variations.

* Corresponding author. University of León (UNILEON), Cellular Biology Area, Campus de Vegazana S/N, CP 24071, León, Spain.
E-mail address: mferrs@unileon.es (M.F. Riesco).
[1] Equal contribution.

https://doi.org/10.1016/j.theriogenology.2023.05.030
0093-691X/

1. Introduction

Artificial insemination in sheep is not very globally widespread due to its irregular and low fertility results [1]. There are several factors intrinsic and extrinsic to the inseminated female that can affect the effectiveness of ovine artificial insemination: farm, year, season, breed, male, ewe age and body condition, reproductive handling, technician, and so on [2]. Among them, it is widely known that the season of insemination have a strong effect on the fertility results [3], even if an hormonal treatment is used to induced and synchronize ewes estrus [4–6]. For males, changes in sexual behavior, hormonal activity, testicular weight and volume, and semen quantity and quality that affect the reproductive performance of rams have been reported [7]. Fertility is a high complex process that depends upon a heterogeneous population of sperm interacting at various levels of the female tract, the vestments of the oocyte, and the oocyte itself [8]. Therefore, male has a direct influence on the fertilization process, as well as on the viability of the preimplantation embryo [9,10]. Classical methods for semen evaluation measured ejaculate volume and sperm cell concentration, sperm gross and progressive motility, and sperm morphology [11]. However, it is generally accepted that conventional sperm characteristics are poorly correlated with the fertilizing capacity of sperm of several species [12–15]. For this reason, laboratory semen evaluation must include the testing of several functional aspects of sperm relevant for fertilization and embryo development, not only in individual sperm but also within a large sperm population as well [16]. In recent years, diverse fluorescent dyes have been used to evaluate several functional characteristics of the sperm cell such as integrity [17], phospholipid transposition [18] and lipid peroxidation [19,20] of the plasmalemma, DNA damage [21,22], apoptosis [23–25], and mitochondrial status [26,27] among others, often assisted by modern flow cytometry that allows rapid counting of a large sperm [28]. New technologies, including genomics, proteomics and, most recently, metabolomics, have been also incorporated in the last decade into the study of sperm biology [29]. Particularly, proteomic analyses of sperm proteins have allowed to understand how sperm acquire their capacity for fertilization and have revealed numerous changes in the sperm proteome related to different variables [30]. This has made possible to identify male fertility biomarkers in several domestic animal species [31–34], new roles of sperm proteins controlling early embryo development [35], new endogenous metabolic pathways [36], and differences in the proteome of ejaculates with high and low motility [37–39] and different ability to withstand preservation by cooling or freezing [40–42]. Changes in the sperm proteome in relation to the sperm preservation protocol have been also described in different species such as ovine [43,44], porcine [45,46], and equine [47]. In addition, studies have carried out on the variations in the sperm proteomic profile at different times of the year in bucks [48], boars [49], and stallions [50]. However, there are no data currently available on how ram sperm proteome varies through the year, and specifically within the mating season.

In this work, 1) we assessed fertility rates after cervical artificial insemination at the beginning (June 21st to July 20th) and at the end (November 20th to December 21st) of the reproductive season in the Assaf breed for the last four years, and 2) we aimed to identify male factors influencing the different reproductive success obtained depending on the time at the mating season in which ovine artificial insemination was performed, with special interest in the proteomic study of ram sperm.

2. Materials and methods

2.1. Ethics statement

The current study was performed according to the Guidelines of the European Union Council (2010/63/EU), following Spanish regulations (RD/1386/2018) for the protection of laboratory animals. All experimental protocols and procedures were approved by the institutional Animal Care and Use Committee of the University of León (ÉTICA-ULE-013-2018).

2.2. Study design

This work was designed to investigate the involvement of ram reproductive and seminal parameters on the differences in fertility rates of Assaf breed in cervical artificial insemination between the beginning (June 21st to July 20th) and the end (November 20th to December 21st) of the breeding season for the last four years. To this end, three levels of evaluation were performed at two very distant points in the mating season (July as Early Breeding Season –EBS– and November as Late Breeding Season –LBS–) (Fig. 1). On a first level, parameters routinely used in ovine reproduction centers such as testicular measurements (in our study total testicular volume), libido, number of sperm doses obtained per male and day of semen collection (calculated from the total daily sperm production) and mass motility were analyzed. In a second level, within the ram evaluation, we performed an ultrasonographic evaluation of testicular blood flow (Resistive and Pulsatility Index) and echotexture (pixels mean gray level, and hypoechoic areas percentage and density). Finally, at the third level, we carried out multiparametric analyses of sperm functionality combined traditional analyses (sperm motility and kinetic parameters by a CASA system) with new ones (sperm quality by flow cytometry), including a sperm proteome study.

2.3. Insemination procedures

Adult Assaf ewes (11,805 females) were subjected to estrus induction and synchronization using intravaginal sponges with 20 mg fluorogestone acetate (Chronogest®, MSD Animal Health, Salamanca, Spain) over 14 days. At sponge withdrawal, ewes were treated with 500 IU of eCG (Folligon®, MSD Animal Health, Salamanca, Spain). Cervical artificial inseminations were performed at 54 ± 2 h after sponge removal. Semen was collected from 246 adult Assaf rams of proven fertility by artificial vagina (water at 40 °C) (IMV Tecnhologies, L'Aigle, France). Only ejaculates with volume ≥ 0.5 mL, mass motility ≥ 4 and sperm concentration ≥ 3,000 × 10^6 sperm/mL were processed. Insemination doses were diluted with INRA 96® diluent (IMV Tecnhologies, L'Aigle, France) at a concentration of 1,600 × 10^6 sperm/mL and slow cooled (−0.5 °C/min) until 15 °C in a programmable water bath (CC-K8, Huber, Germany). Semen was put into French mini-straws (0.25 mL) and held in a transportable refrigerator until arrival at the insemination farm (2–6 h). Cervical artificial inseminations were performed by experienced technicians in the Early Breeding Season (June 21st to July 20th) and in the Late Breeding Season (November 20th to December 21st) for the last four years. Animals were placed with the hindquarter upwards, and the cooled semen (400 × 10^6 sperm) was deposited in the entrance of the cervix using a speculum with an attached light source and an ovine artificial insemination catheter (IMV Tecnhologies, L'Aigle, France). Reproductive success was

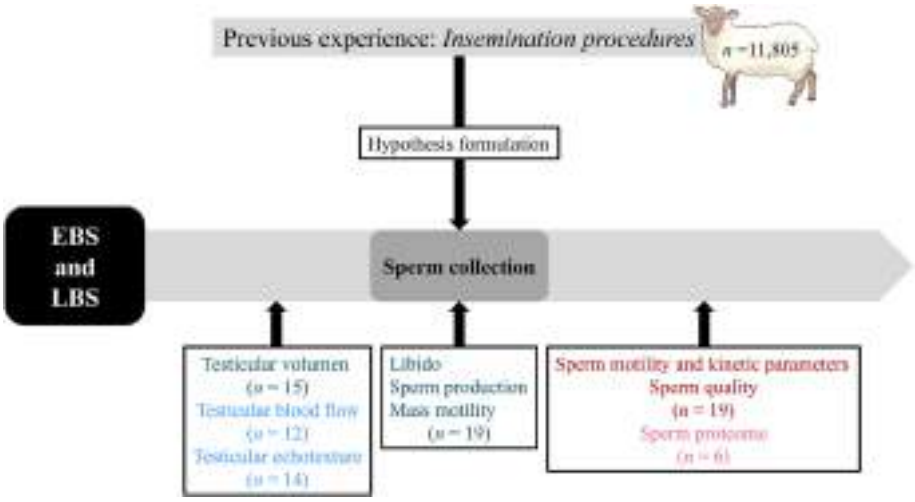

Fig. 1. Study design. Evaluation levels performed in each experimental group (EBS, Early Breeding Season; LBS, Late Breeding Season): **(1)** Reproduction center evaluation: testicular volume, libido, sperm production, and mass motility; **(2)** Ultrasonography evaluation: testicular blood flow and testicular echotexture; **(3)** Sperm functionality evaluation: sperm motility and kinetic parameters, sperm quality, and sperm proteome.

evaluated in terms of fertility according to the total births (including stillbirths) registered at 137–154 days post-insemination.

2.4. Sperm collection and processing

Sperm donors used for the experiment were 19 adult and healthy Assaf rams of proven fertility and trained for semen collection by artificial vagina on a regular basis (weekly semen collections, twice a week). Animals were housed and fed with a standard balanced diet at the Animal Selection and Reproduction Center of the Junta de Castilla y León (CENSYRA, Villaquilambre, León, Spain).

Ram ejaculates (two per male in the same day) were collected in July as Early Breeding Season (EBS) and in November as Late Breeding Season (LBS) by artificial vagina at 40 °C (IMV Technologies, L'Aigle, France) in the presence of a female decoy. Sample tubes were kept in a water bath at 35 °C during the initial evaluation of semen quality. Ejaculate volume was determined using the graduation marks of the collection tube. Mass motility was assessed with a subjective score of 0–5 by a microscope equipped with a warmed stage programmed at 37 °C (Leica DM LB, Meyer Instruments, Houston, TX, USA) using a ×4 objective. Sperm concentration was analyzed by a cell counter (NucleoCounter SP-100, ChemoMetec, Allerod, Denmark). After that, both ejaculates from each male were mixed and diluted down to a final concentration of 1,600 × 10^6 sperm/mL in INRA 96® medium. At this time, samples were refrigerated in a programmable bath using a rate of −0.5 °C/min from 30 °C down to 15 °C. Semen was packed then into 0.25 mL French straws and stored at 15 °C for 6 h.

2.5. Reproduction center evaluation

2.5.1. Testicular volume

Testicular volume of all males was calculated through ultrasound measurements performed by the same technician. All examinations were conducted using a real-time ultrasound scanner (EXAPad®, IMV Tecnhologies, L'Aigle, France) equipped with a 7.5 MHz linear-array transducer. Transducer was covered with a large amount of gel to facilitate ultrasonographic imaging. Scanning was done without pressure to avoid distorting the testicular shape. Images were obtained as caudo-cranial, latero-lateral and ventro-dorsal axis of the testes. Testicular width (W), height (H) and length (L) were measured in triplicate using electronic calipers integrated into the ultrasound machine. Cursors were attached to the edges of the tunica albuginea. Testicular volume was calculated using the formula described by Hedia et al. [51]: W x H x L x 0.71.

2.5.2. Libido

Libido was assessed as previously described Montes-Garrido et al. [52]. Time elapsed from the male contact with the female teaser (a single non-synchronized estrus ewe) until ejaculation was timed in both daily sperm collection and libido was categorized using a 0–10 score. If ejaculation took place in 1 min or less, libido was scored with a value of 10. If ejaculation occurred in 1–2 min, libido obtained a score of 9, and so on. When more than 10 min elapse before ejaculation occurs, libido was scored as 0. Then, the mean of the score obtained in the two seminal collections was calculated.

2.6. Ultrasonography evaluation

2.6.1. Testicular blood flow

As recommended Hassan et al. [53], Doppler parameters were determined at the supratesticular artery in the middle spermatic cord region using a real-time ultrasound scanner equipped with a 10 MHz high-frequency linear-array transducer. Based on previous studies [54–56], angle between the long axis of the vessel and the Doppler beam was set at 35° in the direction of the blood flow. Doppler gate was kept constant at 1 mm. Ultrasound settings (focus, gains, brightness and contrast) were standardized, fixed and used equally for the whole study period to minimize variations. At least three consecutive waveforms were analyzed, and Doppler parameters were automatically calculated by the software package provided with the ultrasound machine. Doppler indices studied were Resistive Index (RI) and Pulsatility Index (PI), which quantify the resistance to blood flow caused by microvascular beds distal to the site of measurement and the pulsatility of oscillations of the waveform, respectively.

2.6.2. Testicular echotexture

Assessments were performed by the same operator using a real-time ultrasound scanner equipped with a linear-array transducer (7.5 MHz). Ultrasound probe was positioned transversely on the

center of each testicle and at least three clips were captured. Ecotext® Software (Humeco, Huesca, Spain) was used for analyzed parenchyma echotexture. Reported echotexture parameters were Test 3 (pixels mean gray level), hypoechoic areas percentage (proportion of the total area occupied by the lumen of the seminiferous tubules in the parenchyma) and hypoechoic areas density (density of seminiferous tubules/cm^2).

2.7. Sperm functionality evaluation

2.7.1. Sperm motility and kinetic parameters by a CASA system

Sperm motility and kinetic assessments were performed using Computer-Assisted Sperm Analysis (CASA) (Sperm Class Analyzer® –SCA– software V 6.3.0.59, Microptic S.L., Barcelona, Spain) set to capture at 100 frames/s a total of 50 frames and particles with an area of 20–70 μm^2. An aliquot of each sperm sample was diluted to a final concentration of 25 × 10^6 sperm/mL in a TES-Tris-Fructose medium supplemented with 1% clarified egg yolk (320 mOsm/kg, pH 7.2) and warmed to 37 °C on a warmed plate for 5 min. Then, 5 μL of the diluted semen was dropped into a Makler counting cell chamber (10 μm depth; Sefi Medical Instruments, Haifa, Israel). Samples were examined with a ×10 negative phase contrast objective in a microscope (Eclipse E400, Nikon, Tokyo, Japan) equipped with a BASLER acA1300-200uc digital camera (Basler Vision Technologies, Ahrensburg, Germany) and a warmed stage (37 °C). At least 400 sperm from four different randomly selected fields were captured and analyzed afterward using the editing facilities provided by SCA. Other events different from sperm were removed, and settings were adjusted in each case to assure a correct tract analysis. Reported kinetics parameters were linearity (LIN, %) and amplitude of the lateral displacement of the sperm head (ALH, μm). Total motility (TM) was defined as the percentage of sperm with curvilinear velocity (VCL) > 15 μm/s and progressive motility (PM) as the percentage of sperm with VCL > 45 μm/s [57].

2.7.2. Sperm quality by flow cytometry

The staining protocol previously described by Riesco et al. [58] was used. Sperm samples were diluted at 2 × 10^6 sperm/mL in phosphate-buffered saline (PBS) (300 mOsm/kg, pH 7.2) in order to wash the cells by short centrifugation (15 s; MiniSpin plus, Eppendorf, Hamburg, Germany). The supernatant was discarded and the sperm pellet was incubated at room temperature and in the dark for 30 min with Zombie Violet™ Fixable Viability Kit (plasma membrane integrity probe) (1:1000 final dilution in PBS; BioLegend, San Diego, CA, USA), CellEvent™ Caspase-3/7 Green Detection Reagent (apoptosis marker) (4 μM final concentration in PBS; ThermoFisher, Waltham, MA, USA) and CellROX™ Deep Red Reagent (reactive oxygen species content labeling) (5 μM final concentration in PBS; Invitrogen, Eugene, OR, USA). After that, another washing step was performed to stop cell staining, and the pellet was resuspended in 1 mL of PBS, carrying out immediately the multiparametric flow cytometry analysis.

Flow cytometry acquisition was performed in a MACSQuant Analyzer 10 (Miltenyi Biotech, Bergisch Gladbach, Germany) equipped with three lasers emitting at 405, 488, and 635 nm (violet, blue and red, respectively) and ten photomultiplier tubes. Violet fluorescence was detected in V1 (excitation 405 nm, emission 450/50 nm), green fluorescence was detected in B1 (excitation 488 nm, emission 525/50 nm), and red fluorescence was detected in R1 (excitation 635 nm, emission 655–730 nm (655LP + split 730)). The system was controlled using MACS Quantify™ software (Miltenyi Biotech, Bergisch Gladbach, Germany) recording a total of 40,000 events per sample and at least 20,000 sperm at a flow rate of 200–300 cells/s. Data were analyzed using FlowJo™ V 10.2 (Ashland, Wilmington, DE, USA).

The interest sperm subpopulations assessed were plotted as follows: viable sperm (Zombie Violet™ low intensity –alive–), apoptotic sperm (CellEvent™ Caspase-3/7 positive) and sperm with high mitochondrial activity (CellROX™ positive).

2.7.3. Sperm proteome analysis

Semen samples from six males were centrifuged at 10,000×*g* for 15 min at 4 °C after being stored at 15 °C for 6 h. Supernatant was discarded and pellet (200 × 10^6 sperm) were kept frozen at −80 °C until analysis. Purity of the samples was checked using phase contrast microscopy. Protein solubilization, quantification and digestion were performed according to the protocol described by Martín-Cano et al. [47]. Briefly, isolated spermatozoa were solubilized in 400 μL of Protein Extraction Reagent Type 4 lysis buffer (Sigma-Aldrich, Saint Louis, MI, USA; 7.0 M urea, 2.0 M thiourea, 40 mM Trizma® base, and 1.0% C7BzO; pH 10.4) and incubated under constant rotation at −4 °C for 1 h. Samples were then centrifuged at 17,000×*g* for 30 min at room temperature to remove cell debris and supernatant was transferred to a new tube. Protein quantification was performed using the 2-D Quant Kit (GE Healthcare, Sevilla, Spain) and 100 μg of protein from each sample were subjected to in-solution trypsin digestion. Analysis of the samples was performed in duplicate with a UHPLC/MS system consisting of an Agilent 1290 Infinity II Series UHPLC (Agilent Technologies, Santa Clara, CA, USA) equipped with an automated multisampler module and a high-speed binary pump, and coupled to an Agilent 6550 Q-TOF Mass Spectrometer (Agilent Technologies, Santa Clara, CA, USA) using an Agilent Jet Stream Dual electrospray (AJS-Dual ESI) interface. The control of the UHPLC and Q-TOF were made by the MassHunter Workstation Data Acquisition software (Rev. B.06.01; Agilent Technologies, Santa Clara, CA, USA). A total of 75 μg of protein per sample were injected into an Agilent AdvanceBio Peptide Mapping UHPLC column (2.7 μm, 150 × 2.1 mm; Agilent Technologies, Santa Clara, CA, USA) thermostatted at 55 °C at a flow rate of 0.4 mL/min. The gradient program started with 2% of B (buffer B: water/acetonitrile/formic acid, 10:89.9:0.1) that remained in isocratic mode for 5 min and then increased linearly up to 45% B in 40 min, increasing up to 95% B in 15 min and remaining constant for 5 min. After this 65 min of run, 5 min of post-time followed using the initial condition for the conditioning of the column for the next run. Mass spectrometer was operated in positive mode. The nebulizer gas pressure was set to 35 psi, whereas the drying gas flow was set to 10 L/min at a temperature of 250 °C, and the sheath gas flow to 12 L/min at a temperature of 300 °C. The capillary spray, fragmentor and octopole RF Vpp voltages were 3,500 V, 340 V and 750 V, respectively. Profile data were acquired for both MS and MS/MS scans in extended dynamic range mode. MS and MS/MS mass range were 50–1,700 *m*/*z* and scan rates were eight spectra/s for MS and three spectra/s for MS/MS. Auto MS/MS mode was used with precursor selection by abundance and a maximum of 20 precursors selected per cycle. A ramped collision energy was used with a slope of 3.6 and an offset of −4.8. The same ion was rejected after two consecutive scans.

Data processing and analysis was performed using Spectrum Mill MS Proteomics Workbench (Rev B.04.01; Agilent Technologies, Santa Clara, CA, USA). Briefly, raw data were extracted under default conditions as follows: non-fixed or variable modifications were selected; [MH] + 50–10,000 *m*/*z*; maximum precursor charge +5; retention time and *m*/*z* tolerance ±60 s; minimum signal-to-noise MS (S/N) 25; finding ^{12}C signals. The MS/MS search against the appropriate and updated protein database (in this case: Uniprot/Sheep) was performed with the following criteria: non-fixed modifications were selected and as variable modification: carbamidomethylated cysteines and tryptic digestion with 5 maximum missed cleavages were selected. ESI-Q-TOF instrument with

minimum matched peak intensity 50%, maximum ambiguous precursor charge +5, monoisotopic masses, peptide precursor mass tolerance 20 ppm, product ion mass tolerance 50 ppm, and calculation of reversed database scores. The autovalidation strategy used was auto-threshold, in which the peptide score is automatically optimized for a target %FDR (False Discovery Rate) of 1.2%. Then, the protein polishing validation was performed in order to increase the sequence coverage of validated results with the restriction of a new maximum target protein %FDR of 0%.

2.8. Bioinformatic analysis of proteomic data

Qlucore Omics Explorer® (Lund, Sweden) was used to compare changes in the relative amounts of proteins based in spectral counts between the EBS and LBS aliquots. Data were Log2 transformed and normalized, and one-way ANOVA was performed filtered by fold change (> 2) with P and q (equivalent to FDR) < 0.05. Results are displayed as means ± SEM. Differences were considered significant when $P < 0.05$. Proteins identified in the EBS and LBS samples were queried for g:Profiler (https://biit.cs.ut.ee/gprofiler/) against the *Ovis aries* database to identify biological pathways likely to be active in ram sperm.

2.9. Statistical analysis

Statistical analysis of fertility data was performed using SAS/STAT® V 9.1 (SAS Institute, Cary, NC, USA), while data from *in vitro* analysis were analyzed using Prism 9 (GraphPad Software, San Diego, CA, USA). Fertility data were analyzed as binomial using the Chi-square test considering the year, farm and male as random factors. Data from *in vitro* analysis were submitted to Levene's and Kolmogorov-Smirnov tests to verify the homogeneity and normality of variables, respectively. Normally distributed data were analyzed by one-way ANOVA, whereas non-normally distributed data were analyzed by Kruskal-Walli's test. The same 12–19 males were analyzed in each experimental group. Results are displayed as mean ± SEM (Standard Error of the Mean). Significant differences were considered at $P < 0.05$.

3. Results

3.1. Insemination procedures

The results of the fertility trial are shown in Table 1. Fertility was significantly lower ($P < 0.0001$) in the EBS than in the LBS.

3.2. Reproduction center evaluation

Quality control assays used in ovine reproduction centers are testicular size, libido, total daily sperm production and mass motility. In this regard, there were non-significant differences ($P \geq 0.05$) in any of these four parameters between the EBS and LBS (Fig. 2).

Table 1
Fertility (lambed ewes/inseminated ewes, %) for the last four years according to the season of insemination.

SEASON	Fertility (%)	Lambed ewes/Total
EBS	28.61[a]	1,388/4,852
LBS	34.69[b]	2,412/6,953

EBS, Early Breeding Season (June 21st to July 20th); LBS, Late Breeding Season (November 20th to December 21st). Different lowercase superscripts letters (a, b) indicate significant differences ($P < 0.0001$) between the EBS and LBS.

3.3. Ultrasonography evaluation

Another factor to consider in order to maximize semen production centers quality control effectiveness is the ultrasound evaluation of the testicular complex. In connection with this, and taking into account the testicular blood flow, both RI and PI Doppler indices were maintained at similar values ($P \geq 0.05$) at the two assessment points (Fig. 3). Concerning to the testicular echotexture, we observed that pixels mean gray level and percentage and density of seminiferous tubules in the testicular parenchyma were similar ($P \geq 0.05$) between the EBS and LBS (Fig. 4).

3.4. Sperm functionality evaluation

Sperm quality after 6 h of liquid storage at 15 °C was similar ($P \geq 0.05$) at both points of the breeding season (Figs. 5 and 6). Only significantly higher sperm viability was observed in the EBS ($P < 0.05$) (Fig. 6A).

3.5. Sperm proteome analysis

Changes in the relative amounts of proteins of samples stored at 15 °C for 6 h as consequence of the timing of the mating season are presented as a heat map (Fig. 7 and Fig. S1). Qlucore Omics Explorer® was used to identify discriminant variables with significant difference between the EBS and LBS samples. 189 proteins with significantly different expression were identified between both moments with a q-value cut-off of 0.094 and a fold change > 2. Interestingly, proteins related to *carbon metabolism*, *citrate cycle (TCA cycle)*, *biosynthesis of amino acids*, *diabetic cardiomyopathy*, and *glycolysis/gluconeogenesis* were decreased at the EBS (Fig. 8). Then, in order to reduce the number of proteins and to obtain fewer proteins with the highest discriminant power between both moments of the reproductive season, those variables with a fold change > 4, P = 2.40e-07, and a q = 2.23e-06 (equivalent to FDR) were selected. The following proteins were identified with the lowest abundance in the EBS (Fig. 9): A0A6P7DP96, A0A6P7DP85, A0A0U1WU05, A0A6P3ERG0, A0A6P7D6E6, A0A6P7E8V0, A0A6P3ET71, A0A835ZRR9, A0A6P3EAP5, A0A6P7ETW8, and A0A6P3EHT6, corresponding to *Fibrous Sheath-Interacting Protein 2*, *Disintegrin and Metalloproteinase Domain-Containing Protein 20-like*, *Phosphoinositide-Specific Phospholipase C*, *Tektin 5*, *Armadillo Repeat-Containing Protein 12 Isoform X3*, *Solute Carrier Family 9B1*, *Radial Spoke Head Protein 3 Homolog*, *Pro-Interleukin-16*, *NADH Dehydrogenase [Ubiquinone] 1 Alpha Subcomplex Subunit 8*, *Testis, Prostate and Placenta-Expressed Protein*, and *Acyl Carrier Protein Mitochondrial*.

4. Discussion

Within temperate latitudes, the breeding season starts during summer or early autumn and ends during the winter in most ovine breeds [59]. As in natural mating, season affects fertility after artificial insemination [60]. Windsor reported low cervical artificial insemination fertility rates in the non-breeding season in Merino ewes [61]. In the same way, Palacín et al. [62] obtained the worse cervical artificial insemination fertility results from March to June and better during the first months of decreasing day length (July and August) in Rasa Aragonesa breed. Our research group previously demonstrated that the season modified the conception rate in Churra ewes after both laparoscopic and vaginal insemination, but also identified differences even within the reproductive season (February–June 43.96 and 29.79%; July–August 38.95 and 22.72%; September–January 46.88 and 35.53%, respectively) [63] as we have done now in the Assaf breed. This effect not only should be

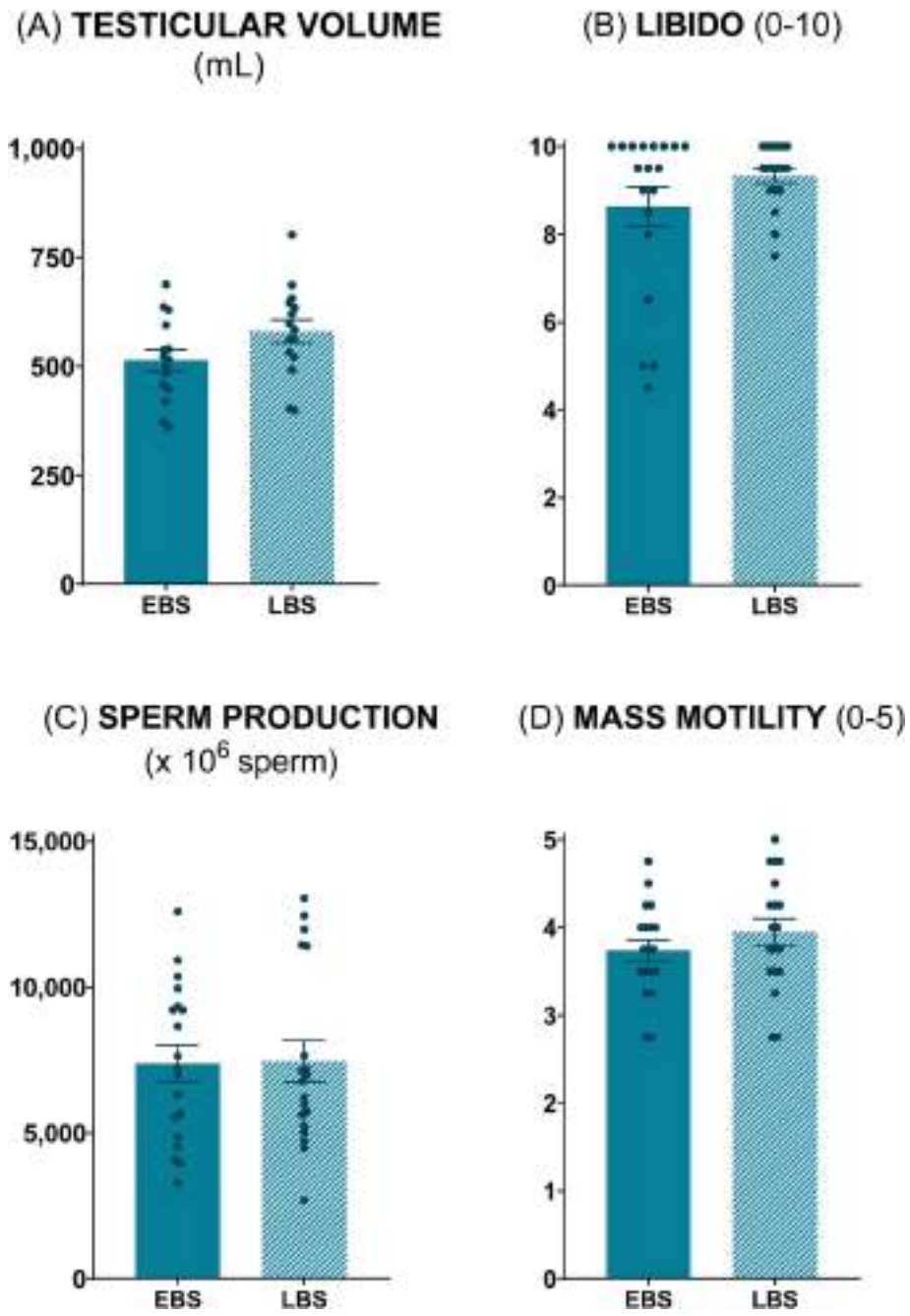

Fig. 2. Ovine reproduction center routine evaluation. **(A)** Total testicular volume (mL)**; (B)** Libido (0–10); **(C)** Total daily sperm production (x 10^6 sperm); **(D)** Mass motility (0–5). The same 15 **(A)** or 19 males **(B, C, D)** were analyzed in each experimental group (EBS, Early Breeding Season; LBS, Late Breeding Season). Graph dots represent the individual values of each ram. Non-significant differences ($P \geq 0.05$) were found between the EBS and LBS.

attributed to the female, since seasonal variations in ram reproductive parameters have been also described [7].

In commercial reproduction centers, the routine andrological evaluations include the determination of testicular dimensions because is considered a valuable index for sperm production assessment in rams [64]. Although conflicting results have been published as regard the highest testicular volume and the time when it is reached, most authors agree that testicular mass increased continuously from the minimum value measured in winter to the maximum recorded in autumn [65–68]. Sexual behavior of rams varies in parallel with changes in testicular size [69], with a peak in summer-autumn and a trough in spring [70]. In our study, both total testicular volume and sperm output as well as libido remained constant from early summer to late autumn, in agreement with previous research conducted on fat-tailed rams in different localities [71–73]. Therefore, we decided to perform an ultrasound evaluation of the testicular complex of the males. Recently, the use of gray-scale ultrasound followed by the application of pulsed-wave Doppler analysis of the testicular artery has widely been conducted to assess the testicular functionality in different species such as rams [74–77], bucks [78], stallions [79], and dogs [80]. Indeed, subjective appearance of the color Doppler image and RI and PI values had been used as diagnostic fertility parameters in camelids [81], stallions [82], dogs [80], and humans

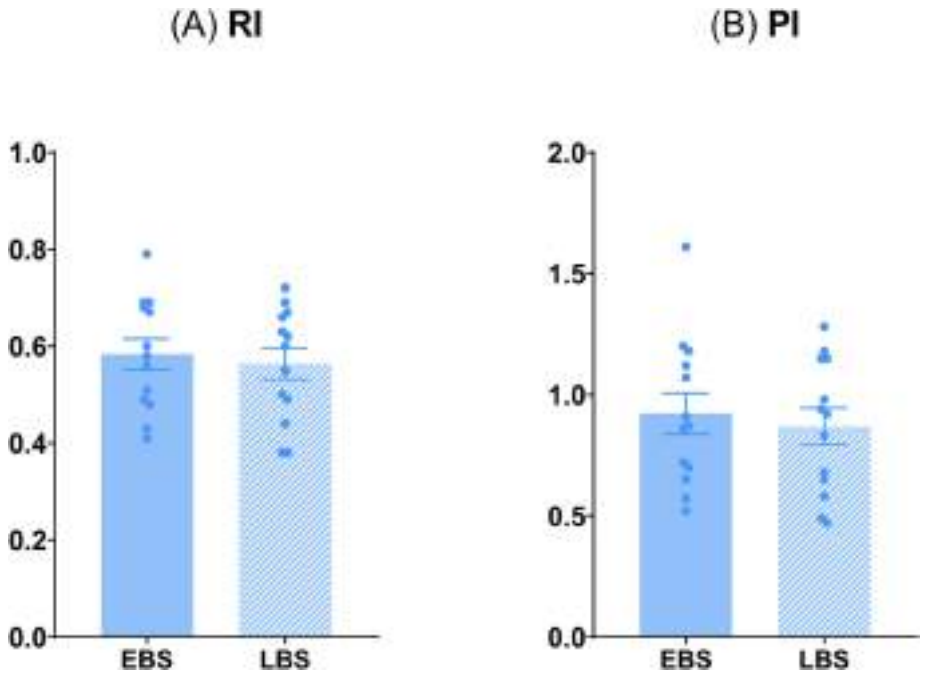

Fig. 3. Ram testicular blood flow evaluation. **(A)** Resistive Index (RI); **(B)** Pulsatility Index (PI). The same 12 males were analyzed in each experimental group (EBS, Early Breeding Season; LBS, Late Breeding Season). Graph dots represent the individual values of each ram. Non-significant differences ($P \geq 0.05$) were found between the EBS and LBS.

[83,84]. Both indices are independent of age, bodyweight, and pulse rate, and therefore, significant changes in their values are usually associated with vascular pathologies [85]. In this work, the overall mean of RI and PI values was stable and comparable to those reported by the previously mentioned studies. Today, previously saved B-mode ultrasound images of testicular parenchyma are analyzed in addition by means of computer-assisted image analysis systems that estimate the numerical pixel intensity values of testicular echogenicity in order to determine tissue density [75,86]. Several studies showed that testicular echotexture had a considerable association with testicular histopathological changes in adult rams [86–88]. However, none of the testicular echotexture parameters studied in our work showed significant differences between the EBS and LBS.

Seasonal variations in ram semen characteristics have been extensively studied, recording the best semen yield in the breeding season [89–91]. Moreover, some reports also determined that monthly fluctuation affects sperm quality in terms of morphology, total and progressive motility, viability, and acrosome integrity [51,71,72]. In this regard, we noticed significant intraseasonal changes only in terms of sperm viability. Surprisingly, the percentage of viable sperm was higher in July than in November, coinciding with the findings of Hedia et al. [92] in fat-tailed Awassi rams under subtropical conditions. In contrast, other study conducted by the same authors using the same experimental conditions showed the lowest percentage of live sperm in July [51], while several authors registered a similar percentage of live cells in summer and autumn in different breeds within the ovine species in studies conducted in the northern hemisphere [66,90,91]. These different trends may be, at least in part, due to breed differences and geographical location. Using proteomic strategies, 189 sperm proteins were identified with a significantly different expression

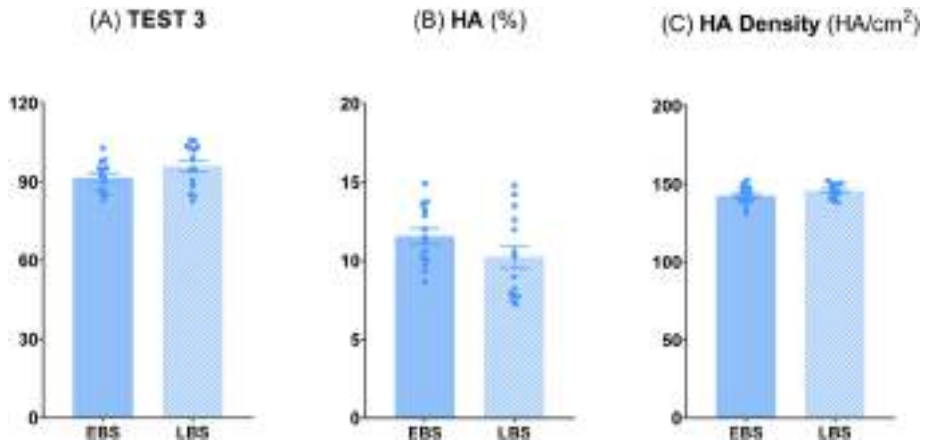

Fig. 4. Ram testicular echotexture evaluation. **(A)** Test 3 (pixels mean gray level); **(B)** hypoechoic areas (HA, %); **(C)** hypoechoic areas density (HA/cm^2). The same 14 males were analyzed in each experimental group (EBS, Early Breeding Season; LBS, Late Breeding Season). Graph dots represent the individual values of each ram. Non-significant differences ($P \geq 0.05$) were found between the EBS and LBS.

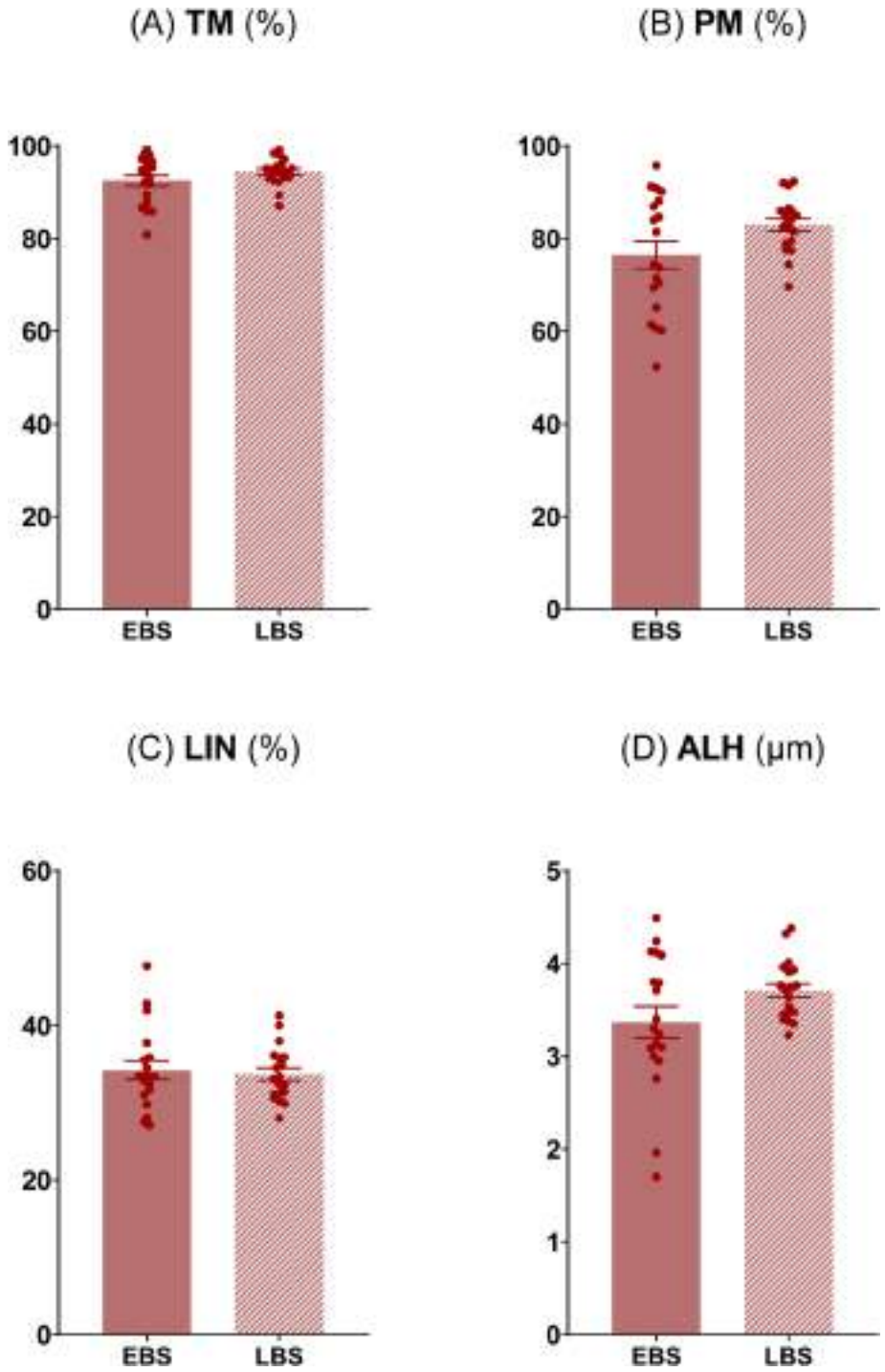

Fig. 5. Ram sperm motility and kinetic evaluation. **(A)** Total motility (TM, %); **(B)** Progressive motility (PM, %); **(C)** Linearity (LIN, %); **(D)** Amplitude of lateral head displacement (ALH, μm). The same 19 males were analyzed in each experimental group (EBS, Early Breeding Season; LBS, Late Breeding Season). Graph dots represent the mixed ejaculates of each ram. Non-significant differences ($P \geq 0.05$) were found between the EBS and LBS.

between the EBS and LBS, and the enrichment analysis revealed that *carbon metabolism*, *citrate cycle (TCA cycle)*, *biosynthesis of amino acids*, *diabetic cardiomyopathy*, and *glycolysis/gluconeogenesis* pathways were less expressed in the EBS. It is well known that mammalian sperm use monosaccharides as the most generalized energy source through both glycolysis (anaerobic pathway) and TCA cycle (aerobic pathway) [93]. However, they can utilize a wide array of substrates to obtain energy such as lactate, pyruvate, citrate [94,95], and glycerol [96]. Our results confirm these previous reports and reveal that ram sperm have a decreased energy metabolism at the start of the reproductive season. The presence of an impaired amino acids synthesis at this time also deserves attention. Recent researches have evidence glutathione (GSH) synthesis in human [97] and stallion sperm [98] after an oxidative insult. One of the consequences of sperm liquid storage is oxidative stress due to redox deregulation caused by an overproduction of ROS and a

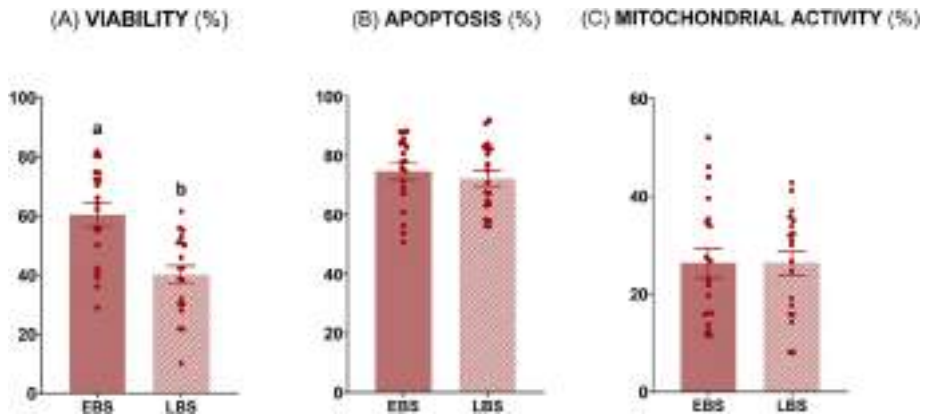

Fig. 6. Ram sperm quality evaluation. **(A)** Viable sperm (%) (Zombie Violet™); **(B)** Apoptotic sperm (%) (CellEvent™ Caspase-3/7 Green); **(C)** Sperm with high mitochondrial activity (%) (CellROX™ Deep Red). The same 19 males were analyzed in each experimental group (EBS, Early Breeding Season; LBS, Late Breeding Season). Graph dots represent the mixed ejaculates of each ram. Different lowercase superscripts letters (a, b) indicate significant differences ($P < 0.05$) between the EBS and LBS.

decrease in the antioxidant capacity of the sample [99]. GSH is the major natural antioxidant protecting cells from oxidative stress [100]. Thus, a decreased GSH synthesis in the EBS could lead to increased oxidative stress, which would inhibit mitochondrial respiration at this time [101,102]. The minor levels of *NADH Dehydrogenase* and *Mitochondrial Acyl Carrier Protein (ACP)* detected with the highest discriminant power in the EBS support these findings. *NADH Dehydrogenase* constitutes complex I, the largest component of the mitochondrial respiratory chain which results in the transfer of electrons from NADH to the electron acceptor ubiquinone thereby providing a proton gradient to produce ATP by ATP synthase [103]. On the other hand, *Mitochondrial ACP* is mainly located in the matrix compartment as a key component of the mitochondrial fatty acid synthesis (FAS) pathway by presenting acyl chain intermediates to catalytic sites of enzymes [104]. In this way, it is required for the production of long-chain fatty acids that are crucial for maintaining phospholipid levels essential for the activity of respiratory complexes II, III, and IV [105]. Furthermore, a small fraction of this protein is integrated into complex I of the electron transport chain [106]. That is, both proteins are necessary for the efficient functioning of the electron transport chain and both of them are down-regulated in the EBS, coinciding with a decreased in energetic metabolism and synthesis of amino acids such as GSH. Within the non-structural proteins with reduced relative abundance in the EBS we also found the *Solute Carrier Family 9B1* (A0A6P7E8V0). In most mammalian species examined, sperm experience a natural increase in intracellular Na^+/HCO_3 concentration and pH value during the journey in the female reproductive tract [107]. This is of great importance for sperm physiology, since it is necessary for further activation of CatSper channels and Ca^{2+} entrance, thus influencing glycolysis and axoneme activity [108,109]. It is known from the literature that two main categories of transmembrane proteins are involved in sperm intracellular pH regulation: bicarbonate and proton carriers [110]. The latter include transporters of the Solute Carrier 9 (SLC9) family, commonly termed Sodium–Hydrogen Exchangers (NHEs) or Antiporters (NHAs), involved in the electroneutral exchange of intracellular H^+ with extracellular Na^+ according to the concentration gradient across the membrane [111]. The SLC9 family is divided into three different subgroups: SLC9A, SLC9B and SLC9C. Specifically, the SLC9B subgroup consists of two recently cloned isoforms: NHA1 (SLC9B1), which is testis-specific, and NHA2 (SLC9B2), which is ubiquitous [110,112,113]. The physiological role of NHA1 and NHA2 is fairly unknown [114], although they appear to have different transport properties. While NHA2 behaves as an electroneutral Na^+/H^+ exchanger, NHA1 is better modeled as an H^+-Cl^- cotransporter [115]. Changes in other two proteins confirm the diminished fertilization ability of ram sperm at the beginning of the reproductive season. According to gene knockout studies in mice [116–119], *Disintegrin and Metalloproteinase Domain-Containing Proteins (ADAMs)* are involved in the binding of sperm to the zona pellucida in the initial gamete adhesion process. However, the binding mechanism is not yet clear. Several studies in mice have suggested that the disintegrin domain of ADAMs bound to particular integrins on the egg plasma membrane [120,121]. On the other hand, crystal structural studies revealed that the hypervariable region in the cysteine-rich domain would serve as an adhesive site [122,123]. In pigs, ADAM20-like expressed on the anterior portion of the plasma membrane was reported to be involved in the adhesion to a specific carbohydrate present in the zona pellucida [124]. The aforementioned function explains our findings, since fertility is lower in EBS, coinciding with a lower expression of this protein. *Phosphoinositide-specific Phospholipase C (PLC)* also plays an essential role in the fertilization process by

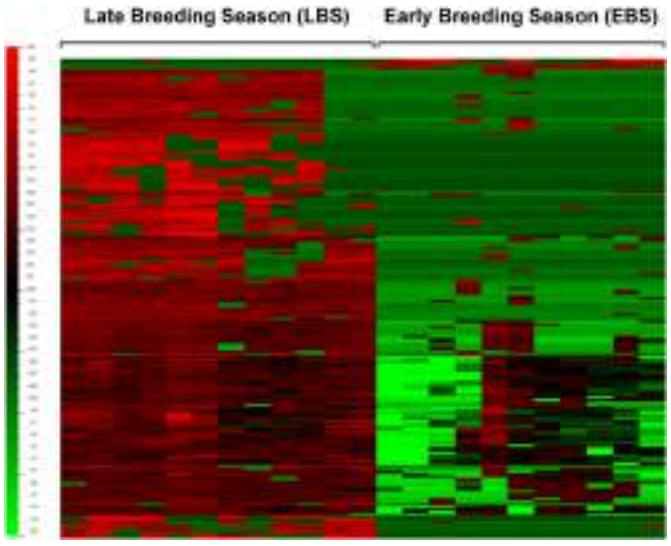

Fig. 7. Heat map showing the impact of the time of the breeding season in the proteome of ram sperm. Proteins are classified following hierarchical clustering. The heat map code is present with red areas representing larger amounts of protein and green areas representing smaller amounts of protein. Proteins were normalized, filtered by a fold change > 2, with P = 0.01 and q = 0.1.

Fig. 8. g:GOST multiquery Manhattan plot showing the enrichment analysis of ram sperm proteins underrepresented in the Early Breeding Season. Kyoto Encyclopedia of Genes and Genomes (KEGG) pathways are depicted in pink. The P values are depicted in the *y* axis and more detailed in the result table below the image.

means of the phosphatidylinositol phosphates (PIPs) metabolism. PLC hydrolyzes phosphatidylinositol 4,5-biphosphate (PIP_2) to generate two second messengers: diacylglycerol (DAG) and inositol 1,4,5-trisphosphate (IP_3). DAG and IP_3 initiate further signal transduction pathways through activation of protein kinase C (PKC) and, in turn, intracellular calcium release [125–127]. Ca^{2+} has a primary role in the execution of the capacitation and acrosomal reaction, an exocytotic event required for fertilization [128], and in the oocyte activation, a fundamental event that initiates embryonic development [129]. The importance of this sperm specific protein has been highlighted by numerous clinical studies directly linking defects or deficiencies in human PLC with documented cases of male infertility [130–134]. Thus, its lower expression in the EBS sperm justifies the lower fertilization rate obtained at this time. A0A6P7ETW8 encodes for *Testis, Prostate and Placenta-Expressed Protein (TEPP)* with uncertain function [135]. *Pro-Interleukin-16 (Pro-IL-16)* is the precursor molecule of the Inlerleukin-16 (IL-16), a pro-inflammatory cytokine originally designated as a lymphocyte chemoattractant factor [136]. However, apart from their role in the immune system modulation, some cytokines are directly involved in the regulation of the testicular function [137]. It has been proposed that they are released by germ, Leydig and Sertoli cells, epididymis and prostate [138], acting as local mediators of the action of sex hormones and paracrine regulators of the spermatogenesis process [139,140]. That is, the lower amount of this protein at the start of the breeding season could influence the course of a successful spermatogenesis. In fact, we also detected changes in four structural proteins of the sperm flagella, a specialized form of

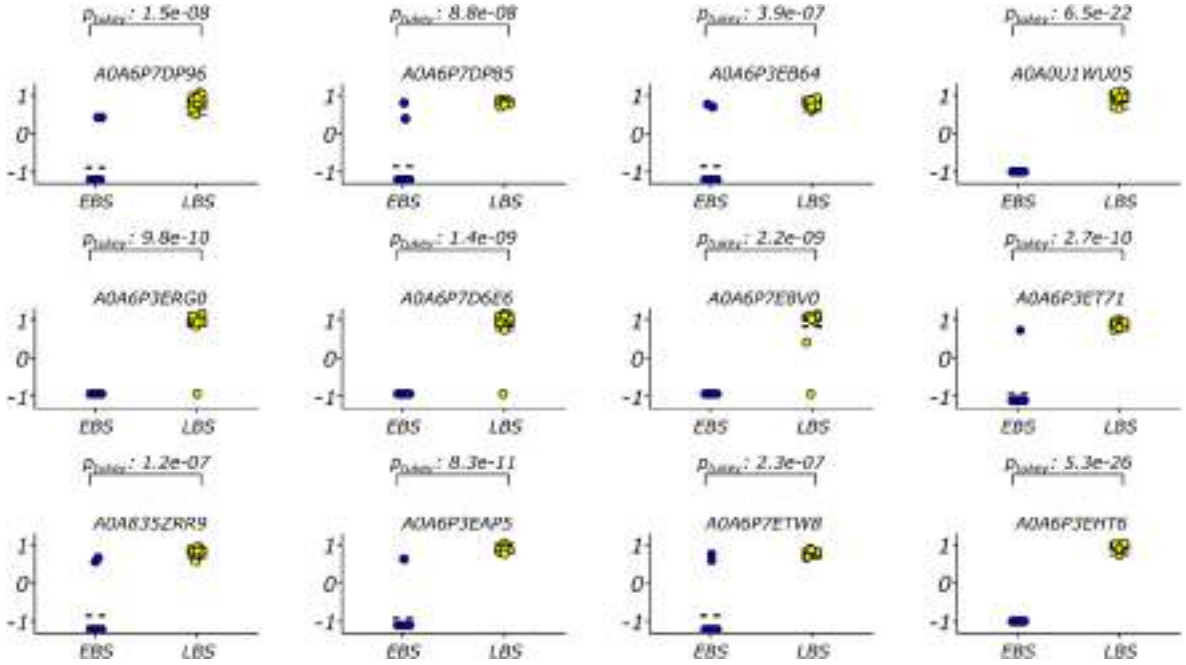

Fig. 9. Qlucore Omics® overrepresentation test of proteins of interest showing a fold change > 4, P = 2.40e-07, and q = 2.23e-06 (equivalent to FDR): A0A6P7DP96, A0A6P7DP85, A0A0U1WU05, A0A6P3ERG0, A0A6P7D6E6, A0A6P7E8V0, A0A6P3ET71, A0A835ZRR9, A0A6P3EAP5, A0A6P7ETW8, and A0A6P3EHT6, corresponding to Fibrous Sheath-Interacting Protein 2, Disintegrin and Metalloproteinase Domain-Containing Protein 20-like, Phosphoinositide-Specific Phospholipase C, Tektin 5, Armadillo Repeat-Containing Protein 12 Isoform X3, Solute Carrier Family 9B1, Radial Spoke Head Protein 3 Homolog, Pro-Interleukin-16, NADH Dehydrogenase [Ubiquinone] 1 Alpha Subcomplex Subunit 8, Testis, Prostate and Placenta-Expressed Protein, and Acyl Carrier Protein Mitochondrial. The same 6 males were analyzed in each experimental group (EBS, Early Breeding Season; LBS, Late Breeding Season). Graph dots represent the individual values of each sample (two technical replicates per male). The P values for each protein are depicted at the top of each plot.

cilium with a structure with more than 1,000 proteins responsible for generating the mechanical force for sperm mobility to reach oocytes in the female genital tract [141]. Sperm flagellum is divided into four parts: connecting, middle, principal, and end pieces. It is composed by the axoneme in its entire length with additional surrounding structures known as peri-axonemal complex, except the end piece which is surrounded by plasma membrane only [142]. Microscopically, the axoneme is a microtubule-based structure consisting of nine outer doublet-microtubules and a central pair that are linked with radial spokes (RSs) and dynein arms. The peri-axonemal complex is composed of outer dense fibers (ODFs), satellite fibrils, and a mitochondrial sheath (MS) in the middle piece [143]. *Tektins (TEKTs)* are constitutive proteins of the axonemal microtubules that seem to be involved in their stability and structural complexity [144]. Five TEKTs (TEKT 1-5) have been identified in mammals so far [144–146]. TEKT 5 is predominantly associated with the inner side of the MS and might work as a middle-piece component requisite for flagellar stability and sperm motility [145]. RSs are T-shaped structures anchored on the outer doublet-microtubules through the spoke stalk (vertical bar of the "T") that transiently interact with the central pair projections using the spoke head (horizontal bar of the "T") [147]. Through studies on *Chlamydomonas reinhardtii*, the purification of the RSs led to the identification of 23 proteins (RSP1–RSP23) [148]. *Radial Spoke Protein 3 (RSP3)* spans and plays a key role in uniting the spoke stalk and head, acting as a core scaffold for RSs and as an anchor to the axoneme [149]. Therefore, defects in this protein are characterized by multiple malformations of the flagella, asthenoteratospermia, and male infertily [150,151]. The *Armadillo Repeat-Containing Protein 12 (ARMC12)* is an outer mitochondrial membrane protein belongs to the ARM family which is evolutionarily conserved among the species and essential for MS formation [152]. Defects in this protein cause morphological abnormalities in the middle piece of sperm flagella in humans [153] and mice [152] resulting, as in the previous case, in asthenoteratospermia and infertility. The principal piece is surrounded by the fibrous sheath (FS), a unique cytoskeletal structure that modulates flagellar bending and defines the shape of the flagellar beat [154]. *Fibrous Sheath-Interacting Protein 2 (FSIP2)* is one of the major components of the FS [155], so is critical for the maintenance of flagellum structure and function [156]. In fact, mutations in FSIP2 have been reported to cause multiple morphological abnormalities of sperm flagella and infertility in humans [156–160]. In addition, FSIP2 has been demonstrated to interact with the A-kinase Anchoring Protein-4 (AKAP4), a crucial enzyme of energy metabolism [161]. Specifically, FSIP2 could play an important role for directing the anchoring of cyclic AMP-dependent Protein Kinase (PKA) to AKAP4, thereby compartmentalizing PKA within the immediate proximity of its enzymatic substrates [162]. Thus, FSIP2 has a vital role on sperm motility and maturation [163,164], and its lower expression in the EBS explains the lower fertilizing capacity of these samples.

In conclusion, while our basic analyses on male and sperm quality showed similar results between the beginning and the end of the breeding season, on a proteomic level we detected a lower expression of sperm proteins linked to the energy metabolism, sperm-oocyte interactions, and flagellum structure in the EBS. Probably, this different protein expression could be related to the lower fertility rate of Assaf ewes after cervical artificial insemination at this time. More importantly, sperm proteins can be used as highly effective molecular markers in predicting sperm fertilization ability related to intraseasonal variations.

Funding

This work is part of the project PID2021-122470OB-I00, supported by MCIN/AEI/10.13039/501100011033/FEDER, UE. Moreover, it is partially financed by MINECO (AGL2017-83098-R) and the University of León. Marta Neila-Montero was supported by MEC (fellowship FPU17/04142), Cristina Palacin-Martinez by MINECO (fellowship PRE2018-086400), and Rafael Montes-Garrido by Junta de Castilla y León and FSE PO 14-20 (fellowship ORDEN EDU/556/2019).

CRediT authorship contribution statement

Every single of the authors has contributed substantially to this manuscript.

Marta Neila-Montero: Conceptualization, Methodology, Software, Validation, Formal analysis, Investigation, Data curation, Writing – original draft, Visualization. **Mercedes Alvarez:** Conceptualization, Validation, Resources, Writing – review & editing, Supervision, Funding acquisition. **Marta F. Riesco:** Conceptualization, Methodology, Validation, Writing – review & editing, Supervision. **Rafael Montes-Garrido:** Conceptualization, Methodology, Validation. **Cristina Palacin-Martinez:** Conceptualization, Methodology, Validation. **Antonio Silva-Rodríguez:** Methodology, Formal analysis. **Francisco E. Martín-Cano:** Methodology. **Fernando J. Peña:** Software, Formal analysis. **Paulino de Paz:** Software, Formal analysis, Resources, Funding acquisition. **Luis Anel:** Conceptualization, Resources, Writing – review & editing, Supervision, Funding acquisition. **Luis Anel-Lopez:** Conceptualization, Validation, Resources, Writing – review & editing, Supervision, Project administration, Funding acquisition.

Declaration of competing interest

The authors declare no conflicts of interest.

Acknowledgments

The authors thank Pedro José de Vega Álvarez and Ainoa Jordán Esteban for their help in the acquisition and analysis of the samples, and the staff of CENSYRA, Ovigén and ASSAF.E for their collaboration in the development of this work.

Appendix A. Supplementary data

Supplementary data to this article can be found online at https://doi.org/10.1016/j.theriogenology.2023.05.030.

References

[1] Anel L, Alvarez M, Martinez-Pastor F, Garcia-Macias V, Anel E, de Paz P. Improvement strategies in ovine artificial insemination. Reprod Domest Anim 2006;41:30–42. https://doi.org/10.1111/j.1439-0531.2006.00767.x.
[2] Martinez-Pastor F, Garcia-Macias V, Alvarez M, Herraez P, Anel L, de Paz P. Sperm subpopulations in Iberian red deer epididymal sperm and their changes through the cryopreservation process. Biol Reprod 2005;72:316–27. https://doi.org/10.1095/biolreprod.104.032730.
[3] Kukovics S, Gyoker E, Nemeth T, Gergatz E. Artificial insemination of sheep - possibilities, realities and techniques at the farm level. Artif. Insemin. Farm Anim., InTech 2011. https://doi.org/10.5772/16642.
[4] deNicolo G, Morris ST, Kenyon PR, Morel PCH. Effect of weaning pre- or post-mating on performance of spring-mated ewes and their lambs in New Zealand. N Z J Agric Res 2006;49:255–60. https://doi.org/10.1080/00288233.2006.9513716.
[5] Ungerfeld R, Rubianes E. Short term primings with different progestogen intravaginal devices (MAP, FGA and CIDR) for eCG-estrous induction in anestrus ewes. Small Rumin Res 2002;46:63–6. https://doi.org/10.1016/S0921-4488(02)00105-0.
[6] Knights M, Baptiste QS, Dixon AB, Pate JL, Marsh DJ, Inskeep EK, et al. Effects of dosage of FSH, vehicle and time of treatment on ovulation rate and prolificacy in ewes during the anestrous season. Small Rumin Res 2003;50:1–9. https://doi.org/10.1016/S0921-4488(03)00111-1.
[7] Casao A, Cebrián I, Asumpção M, Pérez-Pé R, Abecia JA, Forcada F, et al.

Seasonal variations of melatonin in ram seminal plasma are correlated to those of testosterone and antioxidant enzymes. Reprod Biol Endocrinol 2010;8:59. https://doi.org/10.1186/1477-7827-8-59.
[8] Rodríguez-Martínez H. Laboratory semen assessment and prediction of fertility: still Utopia? Reprod Domest Anim 2003;38:312–8. https://doi.org/10.1046/j.1439-0531.2003.00436.x.
[9] Amann RP, DeJarnette JM. Impact of genomic selection of AI dairy sires on their likely utilization and methods to estimate fertility: a paradigm shift. Theriogenology 2012;77:795–817. https://doi.org/10.1016/j.theriogenology.2011.09.002.
[10] Kropp J, Carrillo JA, Namous H, Daniels A, Salih SM, Song J, et al. Male fertility status is associated with DNA methylation signatures in sperm and transcriptomic profiles of bovine preimplantation embryos. BMC Genom 2017;18:1–15. https://doi.org/10.1186/s12864-017-3673-y.
[11] Gadea J. Sperm factors related to in vitro and in vivo porcine fertility. Theriogenology, vol. 63. Elsevier Inc.; 2005. p. 431–44. https://doi.org/10.1016/j.theriogenology.2004.09.023.
[12] Gadea J, Sellés E, Marco M. The predictive value of porcine seminal parameters on fertility outcome under commercial conditions. Reprod Domest Anim 2004;39:303–8. https://doi.org/10.1111/j.1439-0531.2004.00513.x.
[13] Tsakmakidis IA. Ram semen evaluation: development and efficiency of modern techniques. Small Rumin Res 2010;92:126–30. https://doi.org/10.1016/j.smallrumres.2010.04.017.
[14] Petrunkina AM, Waberski D, Günzel-Apel AR, Töpfer-Petersen E. Determinants of sperm quality and fertility in domestic species. Reproduction 2007;134:3–17. https://doi.org/10.1530/REP-07-0046.
[15] Vasan SS. Semen analysis and sperm function tests: how much to test. Indian J Urol 2011;27:41–8. https://doi.org/10.4103/0970-1591.78424.
[16] Tsakmakidis IA. Ram semen evaluation: development and efficiency of modern techniques. Small Rumin Res 2010;92:126–30. https://doi.org/10.1016/j.smallrumres.2010.04.017.
[17] Peña FJ, Saravia F, Johannisson A, Wallgren M, Rodríguez-Martínez H. Detection of early changes in sperm membrane integrity pre-freezing can estimate post-thaw quality of boar spermatozoa. Anim Reprod Sci 2007;97:74–83. https://doi.org/10.1016/J.ANIREPROSCI.2005.12.014.
[18] Gadella BM, Harrison RAP. Capacitation induces cyclic adenosine 3',5'-monophosphate-dependent, but apoptosis-unrelated, exposure of aminophospholipids at the apical head plasma membrane of boar sperm cells. Biol Reprod 2002;67:340–50. https://doi.org/10.1095/BIOLREPROD67.1.340.
[19] Brouwers JFHM, Gadella BM. In situ detection and localization of lipid peroxidation in individual bovine sperm cells. Free Radic Biol Med 2003;35:1382–91. https://doi.org/10.1016/J.FREERADBIOMED.2003.08.010.
[20] Domínguez-Rebolledo Á, Martínez-Pastor F, Fernández-Santos MR, Del Olmo E, Bisbal A, Ros-Santaella JL, et al. Comparison of the TBARS assay and BODIPY C11 probes for assessing lipid peroxidation in red deer spermatozoa. Reprod Domest Anim 2010;45. https://doi.org/10.1111/J.1439-0531.2009.01578.X.
[21] Ribeiro SC, Sartorius G, Pletscher F, De Geyter M, Zhang H, De Geyter C. Isolation of spermatozoa with low levels of fragmented DNA with the use of flow cytometry and sorting. Fertil Steril 2013;100:686–694.e4. https://doi.org/10.1016/J.FERTNSTERT.2013.05.030.
[22] Martínez-Pastor F, Del Rocío Fernández-Santos M, Domínguez-Rebolledo Á, Esteso M, Garde J. DNA status on thawed semen from fighting bull: a comparison between the SCD and the SCSA tests. Reprod Domest Anim 2009;44:424–31. https://doi.org/10.1111/J.1439-0531.2008.01098.X.
[23] Martí E, Pérez-Pé R, Colás C, Muiño-Blanco T, Cebrián-Pérez JA. Study of apoptosis-related markers in ram spermatozoa. Anim Reprod Sci 2008;106:113–32. https://doi.org/10.1016/J.ANIREPROSCI.2007.04.009.
[24] Gil MC, Ferrusola CO, Anel-López L, Ortiz-Rodriguez JM, Alvarez M, de Paz P, et al. A simple flow cytometry protocol to determine simultaneously live, dead and apoptotic stallion spermatozoa in fresh and frozen thawed samples. Anim Reprod Sci 2018;189:69–76. https://doi.org/10.1016/j.anireprosci.2017.12.009.
[25] Skindersoe ME, Kjaerulff S. Comparison of three thiol probes for determination of apoptosis-related changes in cellular redox status. Cytometry 2014;85:179–87. https://doi.org/10.1002/CYTO.A.22410.
[26] Sousa AP, Amaral A, Baptista M, Tavares R, Campo PC, Peregrín PC, et al. Not all sperm are equal: functional mitochondria characterize a subpopulation of human sperm with better fertilization potential. PLoS One 2011;6:e18112. https://doi.org/10.1371/JOURNAL.PONE.0018112.
[27] Marchetti C, Jouy N, Leroy-Martin B, Defossez A, Formstecher P, Marchetti P. Comparison of four fluorochromes for the detection of the inner mitochondrial membrane potential in human spermatozoa and their correlation with sperm motility. Hum Reprod 2004;19:2267–76. https://doi.org/10.1093/HUMREP/DEH416.
[28] Gillan L, Evans G, Maxwell WMC. Flow cytometric evaluation of sperm parameters in relation to fertility potential. Theriogenology 2005;63:445–57. https://doi.org/10.1016/j.theriogenology.2004.09.024.
[29] Long JA. The 'omics' revolution: use of genomic, transcriptomic, proteomic and metabolomic tools to predict male reproductive traits that impact fertility in livestock and poultry. Anim Reprod Sci 2020;220:106354. https://doi.org/10.1016/j.anireprosci.2020.106354.
[30] Kwon W-S, Oh S-A, Kim Y-J, Rahman MS, Park Y-J, Pang M-G. Proteomic approaches for profiling negative fertility markers in inferior boar spermatozoa. Sci Rep 2015;5:13821. https://doi.org/10.1038/srep13821.
[31] Hitit M, Özbek M, Ayaz-Guner S, Guner H, Oztug M, Bodu M, et al. Proteomic fertility markers in ram sperm. Anim Reprod Sci 2021;235:106882. https://doi.org/10.1016/J.ANIREPROSCI.2021.106882.
[32] Peddinti D, Nanduri B, Kaya A, Feugang JM, Burgess SC, Memili E. Comprehensive proteomic analysis of bovine spermatozoa of varying fertility rates and identification of biomarkers associated with fertility. BMC Syst Biol 2008;2:19. https://doi.org/10.1186/1752-0509-2-19.
[33] Muhammad Aslam MK, Sharma VK, Pandey S, Kumaresan A, Srinivasan A, Datta TK, et al. Identification of biomarker candidates for fertility in spermatozoa of crossbred bulls through comparative proteomics. Theriogenology 2018;119:43–51. https://doi.org/10.1016/j.theriogenology.2018.06.021.
[34] Kwon WS, Rahman MS, Lee JS, Yoon SJ, Park YJ, Pang MG. Discovery of predictive biomarkers for litter size in boar spermatozoa. Mol Cell Proteomics 2015;14:1230–40. https://doi.org/10.1074/mcp.M114.045369.
[35] Jodar M, Attardo-Parrinello C, Soler-Ventura A, Barrachina F, Delgado-Dueñas D, Cívico S, et al. Sperm proteomic changes associated with early embryo quality after ICSI. Reprod Biomed Online 2020;40:698–708. https://doi.org/10.1016/j.rbmo.2020.01.004.
[36] Amaral A, Castillo J, Estanyol JM, Ballesca JL, Ramalho-Santos J, Oliva R. Human sperm tail proteome suggests new endogenous metabolic pathways. Mol Cell Proteomics 2013;12:330–42. https://doi.org/10.1074/mcp.M112.020552.
[37] D'Amours O, Frenette G, Bourassa S, Calvo É, Blondin P, Sullivan R. Proteomic markers of functional sperm population in bovines: comparison of low- and high-density spermatozoa following cryopreservation. J Proteome Res 2018;17:177–88. https://doi.org/10.1021/acs.jproteome.7b00493.
[38] Amaral A, Paiva C, Attardo Parrinello C, Estanyol JM, Ballescà JL, Ramalho-Santos J, et al. Identification of proteins involved in human sperm motility using high-throughput differential proteomics. J Proteome Res 2014;13:5670–84. https://doi.org/10.1021/pr500652y.
[39] Griffin RA, Swegen A, Baker M, Aitken RJ, Skerrett-Byrne DA, Rodriguez AS, et al. Mass spectrometry reveals distinct proteomic profiles in high- and low-quality stallion spermatozoa. Reproduction 2020;160:695–707. https://doi.org/10.1530/REP-20-0284.
[40] Gaitskell-Phillips G, Martín-Cano FE, Ortiz-Rodríguez JM, Silva-Rodríguez A, Gil MC, Ortega-Ferrusola C, et al. Differences in the proteome of stallion spermatozoa explain stallion-to-stallion variability in sperm quality post-thaw. Biol Reprod 2021;104:1097–113. https://doi.org/10.1093/biolre/ioab003.
[41] De Lazari FL, Sontag ER, Schneider A, Araripe Moura AA, Vasconcelos FR, Nagano CS, et al. Proteomic identification of boar seminal plasma proteins related to sperm resistance to cooling at 17 °C. Theriogenology 2020;147:135–45. https://doi.org/10.1016/j.theriogenology.2019.11.023.
[42] Rickard JP, Leahy T, Soleilhavoup C, Tsikis G, Labas V, Harichaux G, et al. The identification of proteomic markers of sperm freezing resilience in ram seminal plasma. J Proteonomics 2015;126:303–11. https://doi.org/10.1016/j.jprot.2015.05.017.
[43] Pini T, Rickard JP, Leahy T, Crossett B, Druart X, de Graaf SP. Cryopreservation and egg yolk medium alter the proteome of ram spermatozoa. J Proteonomics 2018;181:73–82. https://doi.org/10.1016/j.jprot.2018.04.001.
[44] He Y, Wang K, Zhao X, Zhang Y, Ma Y, Hu J. Differential proteome association study of freeze-thaw damage in ram sperm. Cryobiology 2016;72:60–8. https://doi.org/10.1016/j.cryobiol.2015.11.003.
[45] Parrilla I, Perez-Patiño C, Li J, Barranco I, Padilla L, Rodriguez-Martinez H, et al. Boar semen proteomics and sperm preservation. Theriogenology 2019;137:23–9. https://doi.org/10.1016/j.theriogenology.2019.05.033.
[46] Perez-Patiño C, Barranco I, Li J, Padilla L, Martinez EA, Rodriguez-Martinez H, et al. Cryopreservation differentially alters the proteome of epididymal and ejaculated pig spermatozoa. Int J Mol Sci 2019;20:1791. https://doi.org/10.3390/ijms20071791.
[47] Martín-Cano FE, Gaitskell-Phillips G, Ortiz-Rodríguez JM, Silva-Rodríguez A, Á Román, Rojo-Domínguez P, et al. Proteomic profiling of stallion spermatozoa suggests changes in sperm metabolism and compromised redox regulation after cryopreservation. J Proteonomics 2020;221. https://doi.org/10.1016/j.jprot.2020.103765.
[48] van Tilburg MF, Salles MGF, Silva MM, Moreira RA, Moreno FB, Monteiro-Moreira ACO, et al. Semen variables and sperm membrane protein profile of Saanen bucks (Capra hircus) in dry and rainy seasons of the northeastern Brazil (3°S). Int J Biometeorol 2014;59:561–73. https://doi.org/10.1007/s00484-014-0869-6.
[49] Martín-Hidalgo D, Macías-García B, García-Marín LJ, Bragado MJ, González-Fernández L. Boar spermatozoa proteomic profile varies in sperm collected during the summer and winter. Anim Reprod Sci 2020;219:106513. https://doi.org/10.1016/j.anireprosci.2020.106513.
[50] Wrench N, Pinto CRF, Klinefelter GR, Dix DJ, Flowers WL, Farin CE. Effect of season on fresh and cryopreserved stallion semen. Anim Reprod Sci 2010;119:219–27. https://doi.org/10.1016/j.anireprosci.2010.02.007.
[51] Hedia MG, El-Belely MS, Ismail ST, Abo El-Maaty AM. Monthly changes in testicular blood flow dynamics and their association with testicular volume, plasma steroid hormones profile and semen characteristics in rams. Theriogenology 2019;123:68–73. https://doi.org/10.1016/j.theriogenology.2018.09.032.
[52] Montes-Garrido R, Riesco MF, Anel-Lopez L, Neila-Montero M, Palacin-Martinez C, Boixo JC, et al. Application of ultrasound technique to evaluate

the testicular function and its correlation to the sperm quality after different collection frequency in rams. Front Vet Sci 2022;9:1869. https://doi.org/10.3389/FVETS.2022.1035036.
[53] Hassan MAA, Sayed RKA, Abdelsabour-Khalaf M, Abd-Elhafez EA, Anel-Lopez L, Riesco MF, et al. Morphological and ultrasonographic characterization of the three zones of supratesticular region of testicular artery in Assaf rams. Sci Rep 2022;12:1–12. https://doi.org/10.1038/s41598-022-12243-z.
[54] Samir H, Sasaki K, Ahmed E, Karen A, Nagaoka K, El Sayed M, et al. Effect of a single injection of gonadotropin-releasing hormone (GnRH) and human chorionic gonadotropin (hCG) on testicular blood flow measured by color Doppler ultrasonography in male Shiba goats. J Vet Med Sci 2015;77:549–56. https://doi.org/10.1292/jvms.14-0633.
[55] Ortega-Ferrusola C, Gracia-Calvo L, Ezquerra J, Pena F. Use of colour and spectral Doppler ultrasonography in stallion andrology. Reprod Domest Anim 2014;49:88–96. https://doi.org/10.1111/rda.12363.
[56] Pozor MA, McDonnell SM. Color Doppler ultrasound evaluation of testicular blood flow in stallions. Theriogenology 2004;61:799–810. https://doi.org/10.1016/S0093-691X(03)00227-9.
[57] Palacin-martinez C, Alvarez M, Montes-Garrido R, Neila-Montero M, Anellopez L, Paz P De, et al. Frequency of semen collection affects ram sperm cryoresistance. Anim an Open Access J from MDPI 2022;12:1492. https://doi.org/10.3390/ani12121492.
[58] Riesco MF, Anel-Lopez L, Neila-Montero M, Palacin-Martinez C, Montes-Garrido R, Alvarez M, et al. ProAKAP4 as novel molecular marker of sperm quality in ram: an integrative study in fresh, cooled and cryopreserved sperm. Biomolecules 2020;10:1046. https://doi.org/10.3390/biom10071046.
[59] Chemineau P, Malpaux B, Delgadillo JA, Guérin Y, Ravault JP, Thimonier J, et al. Control of sheep and goat reproduction: use of light and melatonin. Anim Reprod Sci 1992;30:157–84. https://doi.org/10.1016/0378-4320(92)90010-B.
[60] Santolaria P, Palacin I, Yaniz J. Management factors affecting fertility in sheep. Artif. Insemin. Farm Anim., InTech 2011. https://doi.org/10.5772/18013.
[61] Windsor DP. Factors influencing the success of transcervical insemination in Merino ewes. Theriogenology 1995;43:1009–18. https://doi.org/10.1016/0093-691X(95)00065-G.
[62] Palacín I, Yániz JL, Fantova E, Blasco ME, Quintín-Casorrán FJ, Sevilla-Mur E, et al. Factors affecting fertility after cervical insemination with cooled semen in meat sheep. Anim Reprod Sci 2012;132:139–44. https://doi.org/10.1016/j.anireprosci.2012.05.005.
[63] Anel L, Kaabi M, Abroug B, Alvarez M, Anel E, Boixo JC, et al. Factors influencing the success of vaginal and laparoscopic artificial insemination in churra ewes: a field assay. Theriogenology 2005;63:1235–47. https://doi.org/10.1016/j.theriogenology.2004.07.001.
[64] Toe F, Rege JEO, Mukasa-Mugerwa E, Tembely S, Anindo D, Baker RL, et al. Reproductive characteristics of Ethiopian highland sheep I. Genetic parameters of testicular measurements in ram lambs and relationship with age at puberty in Ewe lambs. Small Rumin Res 2000;36:227–40. https://doi.org/10.1016/S0921-4488(99)00117-0.
[65] Gundoğan M, Demirci E. Monthly changes in some reproductive parameters and in testosterone and thyroxine values of rams throughout one year under continental climate conditions. Dtsch Tierarztl Wochenschr 2003;110:450–3.
[66] Kafi M, Safdarian M, Hashemi M. Seasonal variation in semen characteristics, scrotal circumference and libido of Persian Karakul rams. Small Rumin Res 2004;53:133–9. https://doi.org/10.1016/j.smallrumres.2003.07.007.
[67] Zamiri MJ, Khodaei HR. Seasonal thyroidal activity and reproductive characteristics of Iranian fat-tailed rams. Anim Reprod Sci 2005;88:245–55. https://doi.org/10.1016/j.anireprosci.2004.12.005.
[68] Tajangookeh HD, Shahneh AZ, Shahrebabak MM, Shakeri M. Monthly variation of plasma concentrations of testosterone and thyroid hormones and reproductive characteristics in three breeds of Iranian fat-tailed rams throughout one year. Pakistan J Biol Sci 2007;10:3420–4. https://doi.org/10.3923/pjbs.2007.3420.3424.
[69] Lindsay DR, Pelletier J, Pisselet C, Courot M. Changes in photoperiod and nutrition and their effect on testicular growth of rams. J Reprod Fertil 1984;71:351–6. https://doi.org/10.1530/jrf.0.0710351.
[70] Winfield C, Bremmer W, Cumming I, Galloway D, Making A. Mating behaviour and hormonal changes in rams in relation to breed and season. Proc Aust Soc Anim Prod 1978;12:248.
[71] Zamiri MJ, Khalili B, Jafaroghli M, Farshad A. Seasonal variation in seminal parameters, testicular size, and plasma testosterone concentration in Iranian Moghani rams. Small Rumin Res 2010;94:132–6. https://doi.org/10.1016/j.smallrumres.2010.07.013.
[72] Taha TA, Abdel-Gawad EI, Ayoub MA. Monthly variations in some reproductive parameters of Barki and Awassi rams throughout 1 year under subtropical conditions 1. Semen characteristics and hormonal levels. Anim Sci 2000;71:317–24. https://doi.org/10.1017/S1357729800055168.
[73] Budai C, Oláh J, Egerszegi I, Jávor A, Kovacs A. Seasonal variations in some reproductive parameters of dorper rams in Hungary. Acta Agrar Debreceniensis 2013:17–20. https://doi.org/10.34101/actaagrar/53/2120.
[74] Ntemka A, Kiossis E, Boscos C, Theodoridis A, Kourousekos G, Tsakmakidis I. Effects of testicular hemodynamic and echogenicity changes on ram semen characteristics. Reprod Domest Anim 2018;53:50–5. https://doi.org/10.1111/rda.13279.
[75] Camela ESCC, Nociti RP, Santos VJCC, Macente BI, Murawski M, Vicente WRRR, et al. Changes in testicular size, echotexture, and arterial blood flow associated with the attainment of puberty in Dorper rams raised in a subtropical climate. Reprod Domest Anim 2019;54:131–7. https://doi.org/10.1111/rda.13213.
[76] Batissaco L, Celeghini ECC, Pinaffi FLV, Oliveira BMM de, Andrade AFC de, Recalde ECS, et al. Correlations between testicular hemodynamic and sperm characteristics in rams. Braz J Vet Res Anim Sci 2014;50:384. https://doi.org/10.11606/issn.2318-3659.v50i5p384-395.
[77] Elbaz H, Elweza A, Sharshar A. Testicular color Doppler ultrasonography in Barki rams. Alexandria J Vet Sci 2019;61:39. https://doi.org/10.5455/ajvs.34994.
[78] Kumari S, Luthra RA, Chandolia RK, Pandey AK, Swami DS, Kumar K. Ultrasonographic study of testicular development in Beetal bucks. J Anim Res 2015;5:237. https://doi.org/10.5958/2277-940X.2015.00041.8.
[79] Bollwein H, Schulze JJ, Miyamoto A, Sieme H. Testicular blood flow and plasma concentrations of testosterone and total estrogen in the stallion after the administration of human chorionic gonadotropin. J Reprod Dev 2008;54:335–9. https://doi.org/10.1262/jrd.20014.
[80] Zelli R, Troisi A, Elad Ngonput A, Cardinali L, Polisca A. Evaluation of testicular artery blood flow by Doppler ultrasonography as a predictor of spermatogenesis in the dog. Res Vet Sci 2013;95:632–7. https://doi.org/10.1016/j.rvsc.2013.04.023.
[81] Kutzler M, Tyson R, Grimes M, Timm K. Determination of testicular blood flow in camelids using vascular casting and color pulsed-wave Doppler ultrasonography. Vet Med Int 2011;2011:1–7. https://doi.org/10.4061/2011/638602.
[82] Ortiz-Rodriguez JM, Anel-Lopez L, Martin-Munõz P, Lvarez M, Gaitskell-Phillips G, Anel L, et al. Pulse Doppler ultrasound as a tool for the diagnosis of chronic testicular dysfunction in stallions. PLoS One 2017;12. https://doi.org/10.1371/journal.pone.0175878.
[83] Biagiotti G, Cavallini G, Modenini F, Vitali G, Gianaroli L. Spermatogenesis and spectral echo-colour Doppler traces from the main testicular artery. BJU Int 2002;90:903–8. https://doi.org/10.1046/j.1464-410X.2002.03033.x.
[84] Pinggera G-M, Mitterberger M, Bartsch G, Strasser H, Gradl J, Aigner F, et al. Assessment of the intratesticular resistive index by colour Doppler ultrasonography measurements as a predictor of spermatogenesis. BJU Int 2008;101:722–6. https://doi.org/10.1111/j.1464-410X.2007.07343.x.
[85] Gumbsch P, Gabler C, Holzmann A. Colour-coded duplex sonography of the testes of dogs. Vet Rec 2002;151:140–4. https://doi.org/10.1136/vr.151.5.140.
[86] Giffin JL, Franks SE, Rodriguez-Sosa JR, Hahnel A, Bartlewski PM. A study of morphological and haemodynamic determinants of testicular echotexture characteristics in the ram. Exp Biol Med 2009;234:794–801. https://doi.org/10.3181/0812-RM-364.
[87] Ahmadi B, Lau CP-S, Giffin J, Santos N, Hahnel A, Raeside J, et al. Suitability of epididymal and testicular ultrasonography and computerized image analysis for assessment of current and future semen quality in the ram. Exp Biol Med 2012;237:186–93. https://doi.org/10.1258/ebm.2011.011050.
[88] Giffin JL, Bartlewski PM, Hahnel AC. Correlations among ultrasonographic and microscopic characteristics of prepubescent ram lamb testes. Exp Biol Med 2014;239:1606–18. https://doi.org/10.1177/1535370214543063.
[89] Aller JF, Aguilar D, Vera T, Almeida GP, Alberio RH. Seasonal variation in sexual behavior, plasma testosterone and semen characteristics of Argentine Pampinta and Corriedale rams. Spanish J Agric Res 2012;10:345–52. https://doi.org/10.5424/sjar/2012102-389-11.
[90] Pourseif M. Photoperiod as a factor for studying fluctuations of seminal traits during breeding and non-breeding seasons. J Cell Anim Biol 2012;6:241–9. https://doi.org/10.5897/JCAB12.052.
[91] Moghaddam GH, Pourseif MM, Rafat SA. Seasonal variation in semen quantity and quality traits of Iranian crossbred rams. Slovak J Anim Sci 2012;45:67–75.
[92] Hedia M, El-Belely M, Ismail S, Abo El-Maaty A. Seasonal changes in testicular ultrasonogram pixel-intensity and their association with semen characteristics in rams. Asian Pacific J Reprod 2020;9:49. https://doi.org/10.4103/2305-0500.275635.
[93] Rodriguez-Gil JE. Mammalian sperm energy resources management and survival during conservation in refrigeration. Reprod Domest Anim 2006;41:11–20. https://doi.org/10.1111/j.1439-0531.2006.00765.x.
[94] Jones AR. Metabolism of lactate by mature boar spermatozoa. Reprod Fertil Dev 1997;9:227–32. https://doi.org/10.1071/R96102.
[95] Medrano A, Fernández-Novell JM, Ramió L, Alvarez J, Goldberg E, Rivera MM, et al. Utilization of citrate and lactate through a lactate dehydrogenase and ATP-regulated pathway in boar spermatozoa. Mol Reprod Dev 2006;73:369–78. https://doi.org/10.1002/MRD.20414.
[96] Jones AR, Chantrill LA, Cokinakis A. Metabolism of glycerol by mature boar spermatozoa. Reproduction 1992;94:129–34. https://doi.org/10.1530/JRF.0.0940129.
[97] Evdokimov VV, Barinova KV, Turovetskii VB, Muronetz VI, Schmalhausen EV. Low concentrations of hydrogen peroxide activate the antioxidant defense system in human sperm cells. Biochem 2015 809 2015;80:1178–85. https://doi.org/10.1134/S0006297915090084.
[98] Ortega-Ferrusola C, Martin Muñoz P, Ortiz-Rodriguez JM, Anel-López L, Balao da Silva C, Álvarez M, et al. Depletion of thiols leads to redox deregulation, production of 4-hydroxinonenal and sperm senescence: a possible role for

GSH regulation in spermatozoa. Biol Reprod 2019;100:1090–107. https://doi.org/10.1093/biolre/ioy241.
[99] Mata-Campuzano M, Álvarez-Rodríguez M, Tamayo-Canul J, López-Urueña E, de Paz P, Anel L, et al. Refrigerated storage of ram sperm in presence of Trolox and GSH antioxidants: effect of temperature, extender and storage time. Anim Reprod Sci 2014;151:137–47. https://doi.org/10.1016/J.ANIREPROSCI.2014.10.006.
[100] Lu SC. Glutathione synthesis. Biochim Biophys Acta - Gen Subj 2013;1830:3143–53. https://doi.org/10.1016/J.BBAGEN.2012.09.008.
[101] Alahmar AT. Role of oxidative stress in male infertility: an updated review. J Hum Reprod Sci 2019;12:4–18. https://doi.org/10.4103/jhrs.JHRS_150_18.
[102] Opuwari CS, Henkel RR. An update on oxidative damage to spermatozoa and oocytes. BioMed Res Int 2016;2016. https://doi.org/10.1155/2016/9540142.
[103] Saraste M. Oxidative phosphorylation at the fin de siecle. Science 1999;283:1488–93. https://doi.org/10.1126/science.283.5407.1488. 80.
[104] Masud AJ, Kastaniotis AJ, Rahman MT, Autio KJ, Hiltunen JK. Mitochondrial acyl carrier protein (ACP) at the interface of metabolic state sensing and mitochondrial function. Biochim Biophys Acta - Mol Cell Res 2019;1866:118540. https://doi.org/10.1016/J.BBAMCR.2019.118540.
[105] Guler JL, Kriegova E, Smith TK, Lukeš J, Englund PT. Mitochondrial fatty acid synthesis is required for normal mitochondrial morphology and function in Trypanosoma brucei. Mol Microbiol 2008;67:1125–42. https://doi.org/10.1111/J.1365-2958.2008.06112.X.
[106] Cronan JE, Fearnley IM, Walker JE. Mammalian mitochondria contain a soluble acyl carrier protein. FEBS Lett 2005;579:4892–6. https://doi.org/10.1016/J.FEBSLET.2005.07.077.
[107] Chen S-R, Chen M, Deng S-L, Hao X-X, Wang X-X, Liu Y-X. Sodium-hydrogen exchanger NHA1 and NHA2 control sperm motility and male fertility. Cell Death Dis 2016;7. https://doi.org/10.1038/cddis.2016.65.
[108] Pereira R, Sá R, Barros A, Sousa M. Major regulatory mechanisms involved in sperm motility. Asian J Androl 2015;0:0. https://doi.org/10.4103/1008-682X.167716.
[109] Jō Ao Freitas M, Vijayaraghavan S, Fardilha M. Signaling mechanisms in mammalian sperm motility. Biol Reprod 2017;96:2–12. https://doi.org/10.1095/biolreprod.116.144337.
[110] Martins AD, Bernardino RL, Neuhaus-Oliveira A, Sousa M, Sá R, Alves MG, et al. Physiology of Na+/H+ exchangers in the male reproductive tract: relevance for male Fertility1. Biol Reprod 2014;91:11–2. https://doi.org/10.1095/biolreprod.114.118331.
[111] Fuster DG, Alexander RT. Traditional and emerging roles for the SLC9 Na+/H+ exchangers. Pflugers Arch Eur J Physiol 2014;466:61–76. https://doi.org/10.1007/s00424-013-1408-8.
[112] Xiang M, Feng M, Muend S, Rao R. A human Na+/H+ antiporter sharing evolutionary origins with bacterial NhaA may be a candidate gene for essential hypertension. Proc Natl Acad Sci U S A 2007;104:18677–81. https://doi.org/10.1073/PNAS.0707120104.
[113] Fuster DG, Zhang J, Shi M, Bobulescu IA, Andersson S, Moe OW. Characterization of the sodium/hydrogen exchanger NHA2. J Am Soc Nephrol 2008;19:1547–56. https://doi.org/10.1681/ASN.2007111245.
[114] Yeste M, Recuero S, Maside C, Salas-Huetos A, Bonet S, Pinart E. Blocking NHE channels reduces the ability of in vitro capacitated mammalian sperm to respond to progesterone stimulus. Int J Mol Sci Artic Int J Mol Sci 2021;22:12646. https://doi.org/10.3390/ijms222312646.
[115] Chintapalli VR, Kato A, Henderson L, Hirata T, Woods DJ, Overend G, et al. Transport proteins NHA1 and NHA2 are essential for survival, but have distinct transport modalities n.d. https://doi.org/10.1073/pnas.1508031112.
[116] Cho C, Bunch DOD, Faure JE, Goulding EH, Eddy EM, Primakoff P, et al. Fertilization defects in sperm from mice lacking fertilin β. Science 1998;281:1857–9. https://doi.org/10.1126/science.281.5384.1857. 80.
[117] Shamsadin R, Adham IM, Nayernia K, Heinlein UAO, Oberwinkler H, Engel W. Male mice deficient for germ-cell cyritestin are infertile. Biol Reprod 1999;61:1445–51. https://doi.org/10.1095/biolreprod61.6.1445.
[118] Nishimura H, Kim E, Nakanishi T, Baba T. Possible function of the ADAM1a/ADAM2 fertilin complex in the appearance of ADAM3 on the sperm surface. J Biol Chem 2004;279:34957–62. https://doi.org/10.1074/jbc.M314249200.
[119] Nishimura H, Cho C, Branciforte DR, Myles DG, Primakoff P. Analysis of loss of adhesive function in sperm lacking cyritestin or fertilin β. Dev Biol 2001;233:204–13. https://doi.org/10.1006/dbio.2001.0166.
[120] Bigler D, Takahashi Y, Chen MS, Almeida EAC, Osbourne L, White JM. Sequence-specific interaction between the disintegrin domain of mouse ADAM 2 (fertilin beta) and murine eggs. Role of the alpha(6) integrin subunit. J Biol Chem 2000;275:11576–84. https://doi.org/10.1074/JBC.275.16.11576.
[121] Yuan R, Primakoff P, Myles DG. A role for the disintegrin domain of cyritestin, a sperm surface protein belonging to the ADAM family, in mouse sperm-egg plasma membrane adhesion and fusion. J Cell Biol 1997;137:105–12. https://doi.org/10.1083/JCB.137.1.105.
[122] Takeda S, Igarashi T, Mori H, Araki S. Crystal structures of VAP1 reveal ADAMs' MDC domain architecture and its unique C-shaped scaffold. EMBO J 2006;25:2388–96. https://doi.org/10.1038/sj.emboj.7601131.
[123] Liu H, Shim AHR, He X. Structural characterization of the ectodomain of a disintegrin and metalloproteinase-22 (ADAM22), a neural adhesion receptor instead of metalloproteinase. Insights on adam function. J Biol Chem 2009;284:29077–85. https://doi.org/10.1074/jbc.M109.014258.
[124] Mori E, Fukuda H, Imajoh-Ohmi S, Mori T, Takasaki S. Purification of N-acetyllactosamine-binding activity from the porcine sperm membrane: possible involvement of an ADAM complex in the carbohydrate-binding activity of Sperm. J Reprod Dev 2012;58:117–25. https://doi.org/10.1262/jrd.11-108N.
[125] Majerus PW, Connolly TM, Deckmyn H, Ross TS, Bross TE, Ishii H, et al. The metabolism of phosphoinositide-derived messenger molecules. Science 1986;234:1519–26. https://doi.org/10.1126/SCIENCE.3024320. 80.
[126] Singer WD, Brown HA, Sternweis PC. Regulation of eukaryotic phosphatidylinositol-specific phospholipase C and phospholipase D. Annu Rev Biochem 1997;66:475–509. https://doi.org/10.1146/annurev.biochem.66.1.475.
[127] Rhee SG. Regulation of phosphoinositide-specific phospholipase C. Annu Rev Biochem 2001;70:281–312. https://doi.org/10.1146/annurev.biochem.70.1.281.
[128] Breitbart H. Intracellular calcium regulation in sperm capacitation and acrosomal reaction. Mol Cell Endocrinol 2002;187:139–44. https://doi.org/10.1016/S0303-7207(01)00704-3.
[129] Nomikos M, Kashir J, Lai FA. The role and mechanism of action of sperm PLC-zeta in mammalian fertilisation. Biochem J 2017;474:3659–73. https://doi.org/10.1042/BCJ20160521.
[130] Torra-Massana M, Cornet-Bartolomé D, Barragán M, Durban M, Ferrer-Vaquer A, Zambelli F, et al. Novel phospholipase C zeta 1 mutations associated with fertilization failures after ICSI. Hum Reprod 2019;34:1494–504. https://doi.org/10.1093/humrep/dez094.
[131] Nomikos M, Stamatiadis P, Sanders JR, Beck K, Calver BL, Buntwal L, et al. Male infertility-linked point mutation reveals a vital binding role for the C2 domain of sperm PLCζ. Biochem J 2017;474:1003–16. https://doi.org/10.1042/BCJ20161057.
[132] Escoffier J, Lee HC, Yassine S, Zouari R, Martinez G, Karaouzène T, et al. Homozygous mutation of PLCZ1 leads to defective human oocyte activation and infertility that is not rescued by the WW-binding protein PAWP. Hum Mol Genet 2016;25:878–91. https://doi.org/10.1093/HMG/DDV617.
[133] Kashir J, Konstantinidis M, Jones C, Lemmon B, Chang Lee H, Hamer R, et al. A maternally inherited autosomal point mutation in human phospholipase C zeta (PLCζ) leads to male infertility. Hum Reprod 2012;27:222–31. https://doi.org/10.1093/HUMREP/DER384.
[134] Kashir J, Konstantinidis M, Jones C, Heindryckx B, De Sutter P, Parrington J, et al. Characterization of two heterozygous mutations of the oocyte activation factor phospholipase C zeta (PLCζ) from an infertile man by use of minisequencing of individual sperm and expression in somatic cells. Fertil Steril 2012;98:423–31. https://doi.org/10.1016/J.FERTNSTERT.2012.05.002.
[135] Bera TK, Hahn Y, Lee B, Pastan IH. TEPP, a new gene specifically expressed in testis, prostate, and placenta and well conserved in chordates. Biochem Biophys Res Commun 2003;312:1209–15. https://doi.org/10.1016/J.BBRC.2003.11.031.
[136] Center DM, Cruikshank W. Modulation of lymphocyte migration by human lymphokines. I. Identification and characterization of chemoattractant activity for lymphocytes from mitogen-stimulated mononuclear cells. J Immunol 1982;128:2563–8.
[137] Eggert-Kruse W, Boit R, Rohr G, Aufenanger J, Hund M, Strowitzki T. Relationship of seminal plasma interleukin (IL) -8 and IL-6 with semen quality. Hum Reprod 2001;16:517–28. https://doi.org/10.1093/humrep/16.3.517.
[138] Dousset B, Hussenet F. Les cytokines dans le sperme humain. Une nouvelle voie d'approche de la fertilite masculine, vol. 26. Press Medicale; 1997. p. 24–9.
[139] Takao T, Mitchell WM, Tracey DE, de Souza EB, de Souza EB. Identification of interleukin-1 receptors in mouse testis. Endocrinology 1990;127:251–8. https://doi.org/10.1210/ENDO-127-1-251.
[140] Boockfor FR, Wang D, Lin T, Nagpal ML, Spangelo BL. Interleukin-6 secretion from rat Leydig cells in culture. Endocrinology 1994;134:2150–5. https://doi.org/10.1210/ENDO.134.5.8156916.
[141] Roy A, Yan W, Burns KH, Matzuk MM. Tektin3 encodes an evolutionarily conserved putative testicular microtubules-related protein expressed preferentially in male germ cells. Mol Reprod Dev 2004;67:295–302. https://doi.org/10.1002/MRD.20025.
[142] Kumar N, Singh AK. The anatomy, movement, and functions of human sperm tail: an evolving mystery. Biol Reprod 2021;104:508–20. https://doi.org/10.1093/BIOLRE/IOAA213.
[143] Takiguchi H, Murayama E, Kaneko T, Kurio H, Toshimori K, Iida H. Characterization and subcellular localization of Tektin 3 in rat spermatozoa. Mol Reprod Dev 2011;78:611–20. https://doi.org/10.1002/MRD.21352.
[144] Iida H, Honda Y, Matsuyama T, Shibata Y, Inai T. Tektin 4 is located on outer dense fibers, not associated with axonemal tubulins of flagella in rodent spermatozoa. Mol Reprod Dev 2006;73:929–36. https://doi.org/10.1002/MRD.20486.
[145] Murayama E, Yamamoto E, Kaneko T, Shibata Y, Inai T, Iida H. Tektin5, a new Tektin family member, is a component of the middle piece of flagella in rat spermatozoa. Mol Reprod Dev 2008;75:650–8. https://doi.org/10.1002/MRD.20804.
[146] Wolkowicz MJ, Naaby-Hansen S, Gamble AR, Reddi PP, Flickinger CJ, Herr JC. Tektin B1 demonstrates flagellar localization in human sperm. Biol Reprod 2002;66:241–50. https://doi.org/10.1095/BIOLREPROD66.1.241.
[147] Curry AM, Rosenbaum JL. Flagellar radial spoke: a model molecular genetic system for studying organelle assembly. Cell Motil Cytoskeleton 1993;24:224–32. https://doi.org/10.1002/CM.970240403.

[148] Yang P, Diener DR, Yang C, Kohno T, Pazour GJ, Dienes JM, et al. Radial spoke proteins of Chlamydomonas flagella. J Cell Sci 2006;119:1165–74. https://doi.org/10.1242/jcs.02811.
[149] Gui M, Ma M, Sze-Tu E, Wang X, Koh F, Zhong ED, et al. Structures of radial spokes and associated complexes important for ciliary motility. Nat Struct Mol Biol 2021;28:29–37. https://doi.org/10.1038/S41594-020-00530-0.
[150] Wu H, Wang J, Cheng H, Gao Y, Liu W, Zhang Z, et al. Patients with severe asthenoteratospermia carrying SPAG6 or RSPH3 mutations have a positive pregnancy outcome following intracytoplasmic sperm injection. J Assist Reprod Genet 2020;37:829–40. https://doi.org/10.1007/s10815-020-01721-w.
[151] Jeanson L, Copin B, Papon JF, Dastot-Le Moal F, Duquesnoy P, Montantin G, et al. RSPH3 mutations cause primary ciliary dyskinesia with central-complex defects and a near absence of radial spokes. Am J Hum Genet 2015;97:153. https://doi.org/10.1016/J.AJHG.2015.05.004.
[152] Shimada K, Park S, Miyata H, Yu Z, Morohoshi A, Oura S, et al. ARMC12 regulates spatiotemporal mitochondrial dynamics during spermiogenesis and is required for male fertility. Proc Natl Acad Sci U S A 2021:118. https://doi.org/10.1073/PNAS.2018355118/VIDEO-2.
[153] Liu W, Wei X, Liu X, Chen G, Zhang X, Liang X, et al. Biallelic mutations in ARMC12 cause asthenozoospermia and multiple midpiece defects in humans and mice. J Med Genet 2022;0. https://doi.org/10.1136/JMEDGENET-2021-108137. jmedgenet-2021-108137.
[154] Ricci M, Breed WG. Morphogenesis of the fibrous sheath in the marsupial spermatozoon. J Anat 2005;207:155. https://doi.org/10.1111/J.1469-7580.2005.00437.X.
[155] Brown PR, Miki K, Harper DB, Eddy EM. A-kinase anchoring protein 4 binding proteins in the fibrous sheath of the sperm flagellum. Biol Reprod 2003;68:2241–8. https://doi.org/10.1095/BIOLREPROD.102.013466.
[156] Martinez G, Kherraf ZE, Zouari R, Mustapha SF Ben, Saut A, Pernet-Gallay K, et al. Whole-exome sequencing identifies mutations in FSIP2 as a recurrent cause of multiple morphological abnormalities of the sperm flagella. Hum Reprod 2018;33:1973. https://doi.org/10.1093/HUMREP/DEY264. 84.
[157] Liu W, Wu H, Wang L, Yang X, Liu C, He X, et al. Homozygous loss-of-function mutations in FSIP2 cause male infertility with asthenoteratospermia. J Genet Genomics 2019;46:53–6. https://doi.org/10.1016/J.JGG.2018.09.006.
[158] Liu M, Sun Y, Li Y, Sun J, Yang Y, Shen Y. Novel mutations in FSIP2 lead to multiple morphological abnormalities of the sperm flagella and poor ICSI prognosis. Gene 2021;781. https://doi.org/10.1016/J.GENE.2021.145536.
[159] Hou M, Xi Q, Zhu L, Jia W, Liu Z, Wang C, et al. Novel compound heterozygous mutation in FSIP2 causes multiple morphological abnormalities of the sperm flagella (MMAF) and male infertility. Reprod Sci 2022;29:2697–702. https://doi.org/10.1007/s43032-022-00965-4.
[160] Fang X, Gamallat Y, Chen Z, Mai H, Zhou P, Sun C, et al. Hypomorphic and hypermorphic mouse models of Fsip2 indicate its dosage-dependent roles in sperm tail and acrosome formation. Dev 2021;148. https://doi.org/10.1242/DEV.199216.
[161] Rahamim Ben-Navi L, Almog T, Yao Z, Seger R, Naor Z. A-Kinase Anchoring Protein 4 (AKAP4) is an ERK1/2 substrate and a switch molecule between cAMP/PKA and PKC/ERK1/2 in human spermatozoa. Sci Rep 2016;6:37922. https://doi.org/10.1038/srep37922.
[162] Welch EJ, Jones BW, Scott JD. Networking with AKAPs: context-dependent regulation of anchored enzymes. Mol Interv 2010;10:86. https://doi.org/10.1124/MI.10.2.6.
[163] Eddy EM, Toshimori K, O'Brien DA. Fibrous sheath of mammalian spermatozoa. Microsc Res Tech 2003;61:103–15. https://doi.org/10.1002/jemt.10320.
[164] Eddy EM. The scaffold role of the fibrous sheath. Soc Reprod Fertil Suppl 2007;65:45–62.